JOURNAL OF COMPUTATIONAL PHYSICS 91, 310–343 (1990)

Boundary and Interface Conditions within a Finite Element Preconditioner for Spectral Methods

CLAUDIO CANUTO

Dipartimento di Matematica, Università di Parma, 43100 Parma, Italy and Istituto di Analisi Numerica del C.N.R., corso Carlo Alberto, 5-27100 Pavia, Italy

AND

PAOLA PIETRA

Istituto di Analisi Numerica del C.N.R., corso Carlo Alberto, 5-27100 Pavia, Italy

Received September 19, 1988; revised June 16, 1989

The performances of a finite element preconditioner in the iterative solution of spectral collocation schemes for elliptic boundary value problems is investigated. It is shown how to make the preconditioner cheap by ADI iterations and how to take advantage of the finite element properties in enforcing Neumann and interface conditions in the spectral schemes.

1. INTRODUCTION

Two active fields of current investigation in spectral methods are: (i) the search of efficient solution techniques for the algebraic systems arising from spectral approximations, with an emphasis on those methods which can be advantageously implemented on parallel processors; (ii) the search of efficient and accurate strategies of partitioning the physical domain into simple subdomains, in order to handle complex geometries, nonsmooth solutions or exceedingly large problems. The reader interested in an overview on these topics can refer, e.g., to Chapters 5 and 13 in [2] and the references therein.

The present report aims to bring a contribution to both the themes. We focus on the Helmholtz problem in a d-cube ($d = 2, 3$), subject to different boundary conditions and discretized by a Chebyshev collocation method. We use a finite element preconditioner in solving the collocation scheme by an iterative procedure. As a matter of fact, the starting point of the present investigation has been the paper [6] by Deville and Mund, who first demonstrated numerically the superior preconditioning properties of finite elements over finite differences for spectral systems.

First, we propose an approximate ADI "inversion" of the finite element matrix, which yields nearly as good preconditioning properties as the exact inverse and

0021-9991/90 $3.00

which can be performed in parallel over the row and the columns of the Chebyshev grid. Next, we indicate a mathematically correct formulation of the finite element preconditioner which produces an accurate, unambiguous, and efficient treatment of Neumann boundary conditions, or interface conditions in domain decomposition methods. The proposed method allows one to solve problems with Neumann boundary conditions specified on two or more adjoining sides, or multidomain problems with interior interface corners. The multidomain cost is only slightly larger than the one of a full Dirichlet problem for the same operator in a single domain formulation, with the same number of gridpoints.

An outline of the paper is as follows: Section 2 deals with the description of suitable ADI preconditioners, for the constant coefficient operator in 2D (Subsection 2.1), in 3D (Subsection 2.2), and for the variable coefficient case (Subsection 2.3). The Neumann problem is discussed in Section 3. Finally, the domain decomposition method is presented in Section 4.

2. An ADI-Finite Element Preconditioner

Let us consider the Dirichlet boundary value problem for the Helmholtz operator in the domain $\Omega = (-1, 1)^d$ ($d = 2$ or 3),

$$\begin{aligned} -\Delta U + cU &= f \qquad \text{in} \quad \Omega \\ U &= \Phi \qquad \text{on} \quad \partial\Omega, \end{aligned} \tag{2.1}$$

where $c \geqslant 0$ is a constant and f, Φ are given, smooth data.

In order to define a Chebyshev collocation approximation to this problem, let us introduce a d-uple $N = (N_l)_{l=1,\ldots,d} \in \mathbb{N}^d$ of positive integers, and the corresponding Chebyshev–Lobatto grid in $\bar{\Omega}$

$$G_N = \{\xi = (\xi_l^{(i)})_{l=1,\ldots,d} \mid \xi_l^{(i)} = \cos(i\pi/N_l), \text{ for some } i,\ 0 \leqslant i \leqslant N_l\}. \tag{2.2}$$

Next, let $P_N(\Omega)$ denote the space of the polynomials in Ω of degree up to N_l in the x_l-variable, $1 \leqslant l \leqslant d$. The Chebyshev collocation approximation to the solution U of (2.1) is a polynomial $u = u_N \in P_N(\Omega)$ defined by the set of equations

$$[-\Delta u + cu](\xi) = f(\xi) \qquad \forall \xi \in G_N \cap \Omega, \tag{2.3}$$

$$u(\xi) = \Phi(\xi) \qquad \forall \xi \in G_N \cap \partial\Omega. \tag{2.4}$$

The unknowns are the grid values of u at the points of G_N. The stability and convergence properties of such a numerical approximation have been established in [8] (see also [2, Chap. 11]).

The matrix of the linear system (2.3)–(2.4) is not banded and ill-conditioned. Although the specific constant-coefficient problem (2.3)–(2.4) can be efficiently solved by direct methods based on orthogonal decompositions of the corresponding

matrix (see, e.g., [2, Sect. 5.1], we focus here on iterative methods of solution. Indeed, direct methods become extremely expensive in three space dimensions for large values of N. Furthermore, as discussed in Section 2.3, our approach can be extended to general variable-coefficient problems.

Perhaps the simplest iterative procedure, which has become very popular within spectral methods, is the so-called "preconditioned Richardson iteration," first proposed by Orszag [12]. Starting from an initial point $u^0 \in P_N$ which satisfies the boundary conditions (2.4), a sequence of polynomials $u^k \in P_N(\Omega)$ (individually satisfying (2.4)) is generated by the relation

$$\mathbf{u}^{k+1} = \mathbf{u}^k - \alpha^k A^{-1}(\mathbf{L}_{sp}\mathbf{u}^k - \mathbf{f}), \qquad k = 0, 1, 2, \ldots . \tag{2.5}$$

Here, $\mathbf{u}$ denotes the vector of the gridvalues of the polynomial function u at the interior gridpoints in $G_N \cap \Omega$. Moreover, $\mathbf{L}_{sp}\mathbf{u}^k = -\Delta u^k + cu^k \in P_N(\Omega)$, whereas A stands for an easily invertible approximation of the Helmholtz operator with homogeneous Dirichlet boundary conditions, built-up at the gridpoints of G_N. Finally, α^k is a positive acceleration parameter, which may vary from one iteration to the other. An abundant literature has appeared in recent years, concerned with the choice of the appropriate preconditioner and the acceleration parameter (see, e.g., the discussion given in [2, Sects. 5.2–5.4] and the references therein). In most cases, A is an approximate factorization of the second-order finite difference scheme for the Laplacian on G_N.

The use of a preconditioner based on finite elements rather than finite differences was proposed independently by Canuto and Quarteroni [3], who chose a variational formulation involving the Chebyshev weight $w(\xi) = (1-\xi^2)^{-1/2}$, and by Deville and Mund [6] who preferred the more familiar formulation with constant weight $w(\xi) \equiv 1$. The latter authors gave numerical evidence to the fact that in two space dimensions bilinear finite elements exhibit better preconditioning properties than the five-point finite differences. This improvement is attributed to the property of the finite element method of providing a natural coupling among the algebraic equations to be satisfied at each gridpoint. Another advantage of the finite element method is its easiness in handling Neumann-type boundary conditions. This issue will be adressed in the next sections. Deville and Mund invariably use a direct solver to get the finite element correction at each iteration of (2.5). Hereafter we rather propose an approximate, iterative solver of ADI type.

Let us start by describing in some detail our exact finite element preconditioner. Denote by R_N the collection of rectangles (resp., parallelepipeds) whose vertices are four (resp., eight) neighboring gridpoints of the grid G_N in dimension $d=2$ (resp., $d=3$). Let Q_1 be the space of the polynomials linear in each variable. We introduce the space of the continuous finite element functions

$$V_h = \{v_h \in C^0(\bar{\Omega}) | \forall R \in R_N, v_{h|R} \in Q_1\}. \tag{2.6}$$

Given a continuous function Φ on the boundary of Ω, let $V_h(\Phi)$ be the affine

space of the functions in V_h which coincide with Φ at the boundary nodes of G_N, i.e.,

$$V_h(\Phi) = \{v_h \in V_h \mid v_h(\xi) = \Phi(\xi), \forall \xi \in G_N \cap \partial\Omega\}. \tag{2.7}$$

We set $V_h^0 = V_h(0)$, the linear subspace of V_h of the functions vanishing on the boundary. It is useful to define the following interpolation operators in $\bar{\Omega}$. Let I_h be the Lagrangean finite element interpolator on the grid G_N, i.e.,

$$I_h: C^0(\bar{\Omega}) \to V_h \qquad \text{such that} \quad (I_h v)(\xi) = v(\xi) \qquad \forall \xi \in G_N. \tag{2.8}$$

Denote by I_h^0 the Lagrangean finite element interpolator on G_N, which sets to zero the values of the function on the boundary $\partial\Omega$; i.e.,

$$I_h^0: C^0(\bar{\Omega}) \to V_h^0 \qquad \text{such that} \quad (I_h^0 v)(\xi) = \begin{cases} v(\xi) & \forall \xi \in G_N \cap \Omega \\ 0 & \forall \xi \in G_N \cap \partial\Omega. \end{cases} \tag{2.9}$$

Finally, I_N will be the spectral interpolator on the grid G_N; i.e.,

$$I_N: C^0(\bar{\Omega}) \to P_N(\Omega) \qquad \text{such that} \quad (I_N v)(\xi) = v(\xi) \qquad \forall \xi \in G_N. \tag{2.10}$$

Given a function $F \in L^2(\Omega)$, let us denote by $w_h = A_{fe}^{-1}[F]$ the finite element solution of the following problem

$$w_h \in V_h^0, \qquad \int_\Omega (\nabla w_h \nabla v_h + c w_h v_h) = \int_\Omega F v_h, \qquad \forall v_h \in V_h^0. \tag{2.11}$$

The preconditioned Richardson iterations are defined as follows: the starting point is chosen to be the spectral interpolant of the finite element approximation to the Dirichlet boundary problem (2.1); i.e., we set $u^0 = I_N w_h^0$, where w_h^0 satisfies

$$w_h^0 \in V_h(\Phi), \qquad \int_\Omega (\nabla w_h^0 \nabla v_h + c w_h^0 v_h) = \int_\Omega f v_h, \qquad \forall v_h \in V_h^0. \tag{2.12}$$

The subsequent interations are defined via the formula

$$u^{k+1} = u^k - \alpha^k I_N A_{fe}^{-1}[I_h^0(L_{sp} u^k - f)], \tag{2.13}$$

where α^k is an acceleration parameter, whose choice will be discussed in the sequel.

Formula (2.13) is a functional formulation of the Richardson iterations, since the equality sign is between polynomials in P_N. Readers more familiar with a matrix formulation, can think of (2.13) as

$$\mathbf{u}^{k+1} = \mathbf{u}^k - \alpha^k (S + cM)^{-1} M(\mathbf{L}_{sp} \mathbf{u}^k - \mathbf{f}). \tag{2.14}$$

As before, $\mathbf{u}$ denotes the vector of the interior gridvalues of the function $\mathbf{u}$ in Ω. S is the stiffness matrix associated with the finite element approximation to the

Laplace operator with homogeneous boundary conditions. M is the corresponding mass matrix, acting on the interior gridvalues only.

The formulation given so far assumes that each finite element system, such as (2.11) or (2.13), is solved exactly. In practice, an approximate solution of these systems will be enough to ensure good preconditioning properties. Taking advantage of the tensor-product structure of our problem, we propose to solve the system (2.11) (and (2.12)), by an alternating direction iterative (ADI) method. Thus, denoting now by $w_h = \mathscr{A}_{fe}^{-1}[F]$ the approximate solution of (2.11) obtained by a fixed number of ADI sweeps starting from the initial value $w_h^{(0)} = 0$, (2.13) becomes

$$u^{k+1} = u^k + \alpha^k I_N \mathscr{A}_{fe}^{-1}[I_h^0(L_{sp}u^k - f)]. \tag{2.15}$$

The initial point of this iterative procedure is also computed by a fixed number of ADI sweeps applied to (2.12).

In the rest of the section, we briefly describe ADI procedures for solving the algebraic system

$$(S + cM)\, w = MF \tag{2.16}$$

corresponding to (2.11). Moreover, we discuss their theoretical and practical performances as preconditioners in the iterative scheme (2.15). Finally, we indicate how to extend the methods to variable coefficient problems. From now on the 2D case and the 3D case will be treated separately.

2.1. *Two-Dimensional Problems*

We consider the ADI method proposed by Douglas and Dupont [5]. Set $N = (N_x, N_y)$ and $(x_1, x_2) = (x, y)$. Let $\alpha_i(x)$, $i = 0, ..., N_x$ be the continuous function in $[-1, 1]$, piecewise linear on the mesh generated by the grid points $\{x_k = \cos(k\pi/N_x),\ k = 0, ..., N_x\}$ such that $\alpha_i(x_j) = \delta_{ij}$, $j = 0, ..., N_x$ (δ_{ij} denotes the Kronecker index). Let $\beta_j(y)$, $j = 0, ..., N_y$ be defined similarly. Then

$$M = M_x \otimes M_y, \qquad S = S_x \otimes M_y + M_x \otimes S_y \tag{2.17}$$

where the symbol $\otimes$ denotes the familiar tensor product between matrices, and

$$M_x = \left\{\int_{-1}^{1} \alpha_i(x)\, \alpha_k(x)\, dx\right\}_{i,k=1,...,N_x-1} \qquad M_y = \left\{\int_{-1}^{1} \beta_j(y)\, \beta_l(y)\, dy\right\}_{j,l=1,...,N_y-1}$$

$$S_x = \left\{\int_{-1}^{1} \alpha_i'(x)\, \alpha_k'(x)\, dx\right\}_{i,k=1,...,N_x-1} \qquad S_y = \left\{\int_{-1}^{1} \beta_j'(y)\, \beta_l'(y)\, dy\right\}_{j,l=1,...,N_y-1}. \tag{2.18}$$

Set

$$A_x = S_x + \frac{c}{2} M_x, \qquad A_y = S_y + \frac{c}{2} M_y,$$

and denote by I_x (resp., I_y) the identity matrix of order $(N_x - 1)$ (resp., $(N_y - 1)$).

We introduce the new unknown $\xi = I_x \otimes M_y \mathbf{w}$ and $\eta = I_y \otimes M_x \tilde{\mathbf{w}}$, where $\tilde{\mathbf{w}}$ is obtained by reversing the row–column ordering of $\mathbf{w}$, and we proceed as follows: given $\mathbf{w}^0$, set $\eta^0 = I_y \otimes M_x \tilde{\mathbf{w}}^0$; then, compute the general step:

$$I_y \otimes (M_x + \Delta t^{n+1} A_x)\, \xi^{n+1/2} = \Delta t^{n+1} M_x \otimes M_y \mathbf{F} + I_x \otimes (M_y - \Delta t^{n+1} A_y)\, \eta^n;$$
$$I_x \otimes (M_y + \Delta t^{n+1} A_y)\, \eta^{n+1} = \Delta t^{n+1} M_x \otimes M_y \mathbf{F} + I_y \otimes (M_x - \Delta t^{n+1} A_x)\, \xi^{n+1/2}. \tag{2.19}$$

Finally, after the last iteration, recover $\mathbf{w}$ from η by solving

$$\tilde{\mathbf{w}} = I_y \otimes M_x^{-1} \eta. \tag{2.20}$$

Each one of the previous systems is indeed a collection of linear systems acting on the unknows of one row or one column of the grid. Thus, they can be solved by a parallel procedure. The corresponding matrices are tridiagonal. So, the computational amount of work per sweep is the solution of $2(N_y - 1)$ (resp., $2(N_x - 1)$) triangular systems, plus one LU factorization of a $(N_x - 1) \times (N_x - 1)$ and a $(N_y - 1) \times (N_y - 1)$ tridiagonal matrix which can be done once for all. At the beginning a matrix–vector multiplication has to be performed, whereas at the end the system (2.20) has to be solved. Note that, although bilinear finite elements lead to algebraic equations involving nine neighboring unknowns, the computational effort of the ADI procedure is essentially the same as the one required for solving the familiar five-point finite difference approximations with an iterative scheme of the same kind.

It is known that a fast convergence of an ADI scheme requires proper selection of the parameters $\{\Delta t^n\}$. Following [13], we pick a cyclic geometric sequence of $\{\Delta t^n\}$ of prescribed cycle length LC (the effective choice of Δt^n and LC are recalled in the Appendix, formulae (A.9)-(A.11)). With such a choice, an error reducton by a factor ε can be obtained with $O(\log(\rho_{\max}/\rho_{\min})) \cdot O(\log \varepsilon^{-1})$ iterations, where $\rho_{\max}$ and $\rho_{\min}$ are the maximum and minimum eigenvalues of the one-dimensional finite element matrices. For the Chebyshev grid, $\rho_{\max}/\rho_{\min} = O(N^4)$, where $N = \max(N_x, N_y)$. Thus, the number of ADI iterations needed to reach a prescribed accuracy in solving problem (2.11) grows only logarithmically with the number of gridpoints. This fact has the following effect on the preconditioning of the spectral matrix L_{sp}: Denote here by $A_{fe} = M^{-1}(S + cM)$ the matrix corresponding to the exact finite element problem (2.11), and let $\mathscr{A}_{fe}$ be its approximation obtained by performing one cycle of length LC of ADI iterations. Then, the modulus κ of the ratio of largest to smallest eigenvalue of $\mathscr{A}_{fe}^{-1} L_{sp}$ obeys a law of the type

$$\kappa(\mathscr{A}_{fe}^{-1} L_{sp}) \simeq \frac{\kappa(A_{fe}^{-1} L_{sp})}{1 - \varepsilon}, \tag{2.21}$$

where ε is the error reduction factor corresponding to the cycle length LC (we will

prove the previous relation in Appendix A, under the assumption of periodic boundary conditions). It is known (see [6] and Appendix A) that $\kappa(A_{fe}^{-1} L_{sp})$ is bounded independently of N. Thus, the same property holds for the matrix $\mathscr{A}_{fe}^{-1} L_{sp}$, provided the cycle length LC is increased at a logarithmic rate in the number of gridpoints.

Let us now briefly discuss the computational cost of the ADI-preconditioned method (2.19). For the sake of simplicity we assume here that $N_x = N_y = N$. The cost of one ADI step is asymptotic with $12\,N^2$ operations as $N \to \infty$ (if the factorization of the tridiagonal matrices is performed and stored once for all). On the other hand, the cost of computing the spectral residual $L_{sp} u - f$ is asymptotic with $10\,N^2 \log_2 N$ operations, since one discrete Chebyshev transform can be performed in $5/2\ N^2 \log_2 N + 11N^2$ operations as $N \to \infty$. We conclude that a fixed reduction in the relative residual can be obtained in $O(N^2 \log_2 N)$ operations. The reader should also take into account that our iterative method can be completely parallelized on the rows and columns of the mesh.

Finally, a few words about the choice of the acceleration parameter α^k. It can be kept fixed throughout the iterations, or chosen at each iteration in order to minimize a suitable norm of the residual. In the latter case, we shall minimize the discrete L^2-norm (at the interior grid points of G_N) of the preconditioned residual

$$\text{res}^{k+1} = \mathscr{A}_{fe}^{-1} [I_h^0 (L_{sp} u^{k+1} - f)], \tag{2.22}$$

since this expression can be easily generalized to the case of Neumann boundary conditions. We shall denote by MR (minimal residual) this strategy of dynamically choosing the acceleration parameter.

Numerical Results. We present hereafter some numerical experiences concerning the finite element ADI preconditioner described above. As a test problem, we chose $U(x, y) = \sin 2\pi x \cos 2\pi y$ and $c = 0$ in (2.1).

Figure 1 shows the convergence histories of the iterative scheme (2.15) in which $\alpha^k = 1$, for two diffeent values of the grid parameter N. The logarithm of the discrete l^2 norm of the preconditioned residual (2.22) is plotted versus the number of iterations, for several choices of the ADI cycle length LC. Shown is also the convergence of the iterative scheme (2.13) which uses the exact finite element preconditioner. The results confirm our prediction that the error reduction per iteration is essentially independent of N if the cycle length is chosen according to the logarithmic law described above.

In the previous experiments we used one cycle of ADI sweeps per Richardson iterations. In Fig. 2a we compare the behavior of the residual when the number NC of ADI cycles per Richardson iteration is increased, but the length is kept fixed. It appears that the gain in speed produced by this strategy is not enough to compensate for the increase in cost (by a factor 3) for solving the preconditioning problem at each Richardson iteration. Fig. 2b shows that for the same cost it is more effective to use one long cycle of ADI parameters rather than several short cycles.

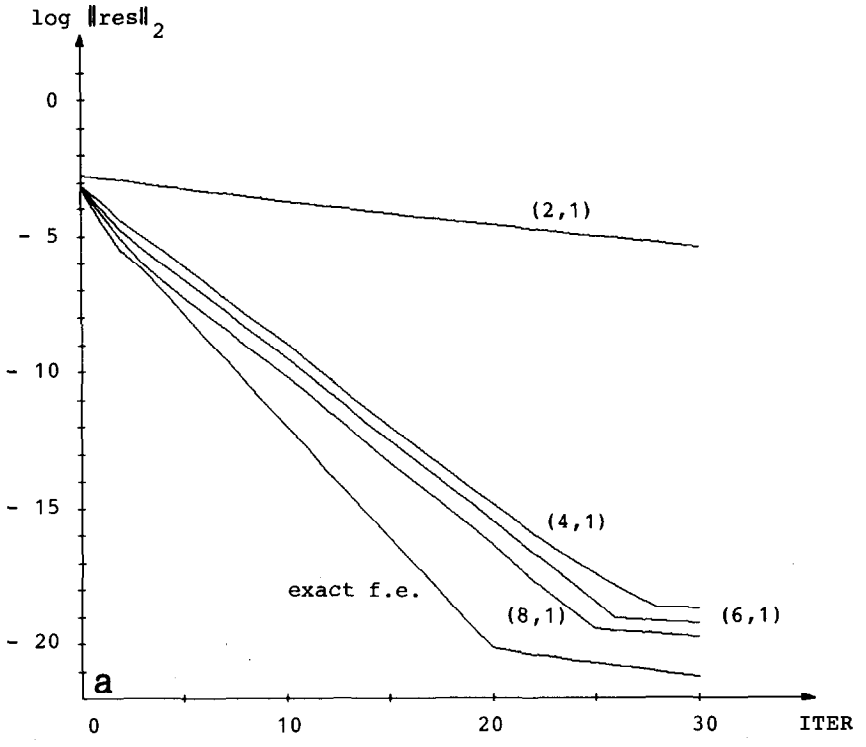

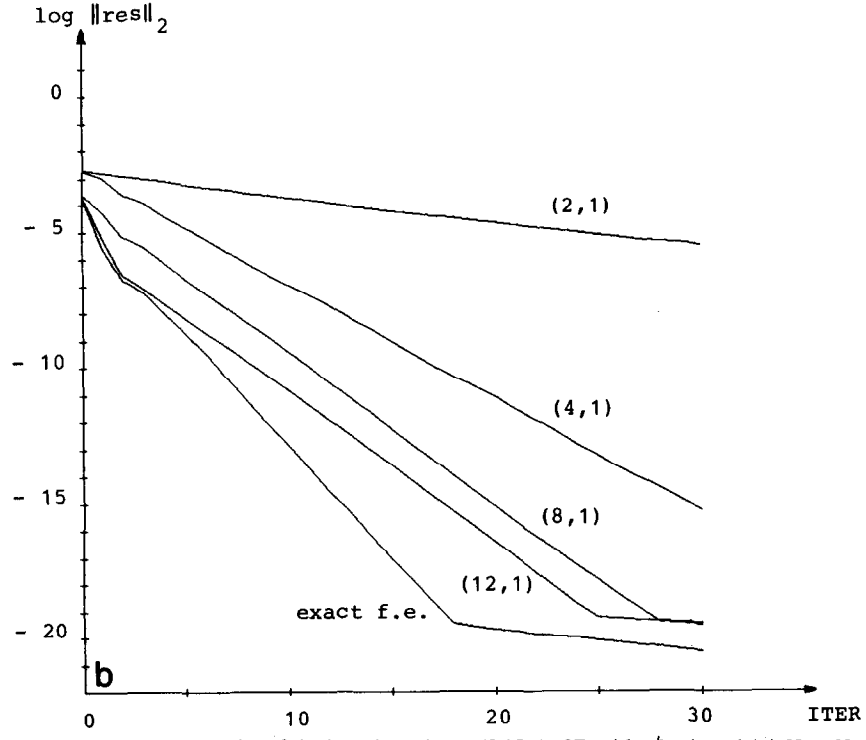

FIG. 1. Convergence histories of the iterative scheme (2.15) in 2D with $\alpha^k \equiv 1$. and (a) $N_x = N_y = 16$; or (b) $N_x = N_y = 32$, for different ADI parameters (LC, NC). Shown is also the convergence history of (2.13) ("exact f.e.").

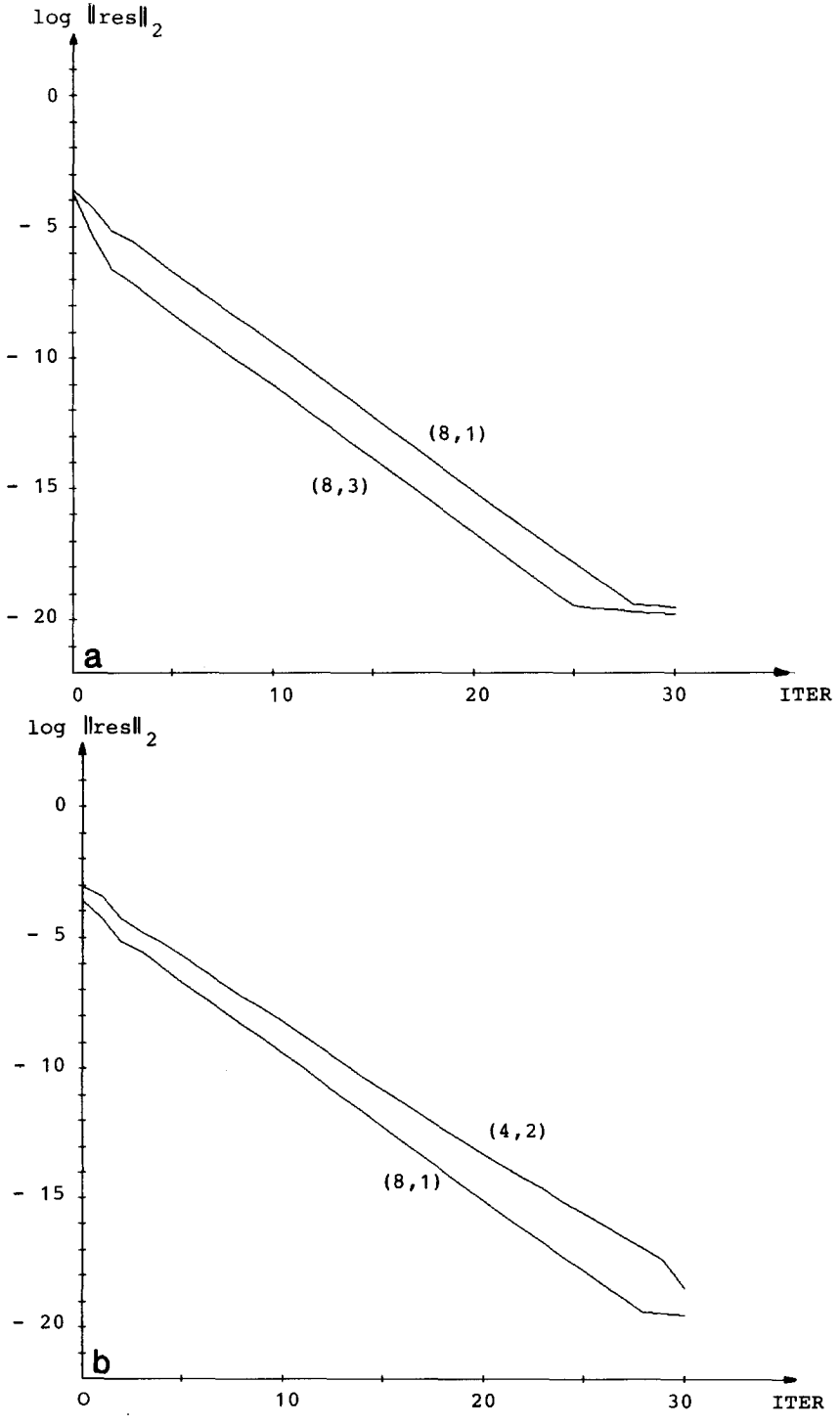

FIG. 2. Convergence histories of (2.15) in 2D with $\alpha^k = 1.$ and $N_x = N_y = 32$: sensitiveness to the ADI parameters (*LC*, *NC*).

Finally, in Fig. 3 we compare the convergence histories obtained with a fixed acceleration parameter and with the dynamically chosen parameter, according to the MR strategy. Unlike the case of finite difference preconditioners (see, e.g., [3]), the difference in the speed of convergence is moderate. Note that $\alpha = 1$ is *not* the optimal value which maximizes the minimal error reduction factor (see [12]); other nearby values yield a better convergence speed, but we have deliberately avoided a trial and error search. The similarity in the behavior of the two strategies for choosing the acceleration parameter confirm the better preconditioning properties of finite elements. This fact was first pointed out by Deville and Mund [6], who used a direct solution of the finite element system. Here we observe the same property when a cheaper, approximate solver is employed.

Figure 3 also allows us to compare the performance of our finite element preconditioner with the one of the finite difference five-diagonal incompletely factorized matrix $\mathscr{A}_{fd}$ proposed in [14]. Using in both cases the MR strategy in finding α^k, our preconditioner gives a faster speed of convergence by a factor of 2.8 for $N = 16$ and by a factor of 3.6 for $N = 32$. On the other hand, the cost of one Richardson iteration (2.15) is $(12LC + 10 \log_2 N) N^2$ (where LC is the ADI cycle length) for the method proposed here, and is $(5 + 10 \log_2 N) N^2$ for the [14] method. Hence, the cost ratio per iteration is 2.5 when $N = 16$ ($LC = 6$) and 2.7 when $N = 32$ ($LC = 8$). We recall that the condition number κ of the matrix $\mathscr{A}_{fd}^{-1} L_{sp}$ grows like $\sqrt{N}$ (see [14]); hence, a fixed reduction in the relative residual is achieved by the [14] method in $O(N^2 \sqrt{N})$ operations. This must be compared with the $O(N^2 \log_2 N)$-ops cost of our method. Moreover, as already pointed out, our preconditioner is fully parallelizable.

2.2. *Three-Dimensional Problems*

By extending the notation of Section 2.1 to three dimensions in an obvious way, the mass and stiffness matrices in (2.17) now take the form

$$M = M_x \otimes M_y \otimes M_z, \qquad S = S_x \otimes M_y \otimes M_z + M_x \otimes S_y \otimes M_z + M_x \otimes M_y \otimes S_z. \tag{2.23}$$

It is known that the straightforward generalization of (2.19) to three space variables is unstable. Among the possible 3D splittings (see, e.g., Yanenko [18]), we have chosen the ADI splitting proposed by Douglas [4], for its properties of consistency with the exact operator and strong stability. Thus, we set

$$A_x = S_x + \tfrac{1}{3} c M_x, \qquad A_y = S_y + \tfrac{1}{3} c M_y, \qquad A_z = S_z + \tfrac{1}{3} c M_z \tag{2.24}$$

and we introduce the new variables

$$\xi = I_x \otimes M_y \otimes M_z \mathbf{w}, \qquad \eta = I_y \otimes M_x \otimes M_z \tilde{\mathbf{w}}, \qquad \zeta = I_z \otimes M_x \otimes M_y \bar{\mathbf{w}}, \tag{2.25}$$

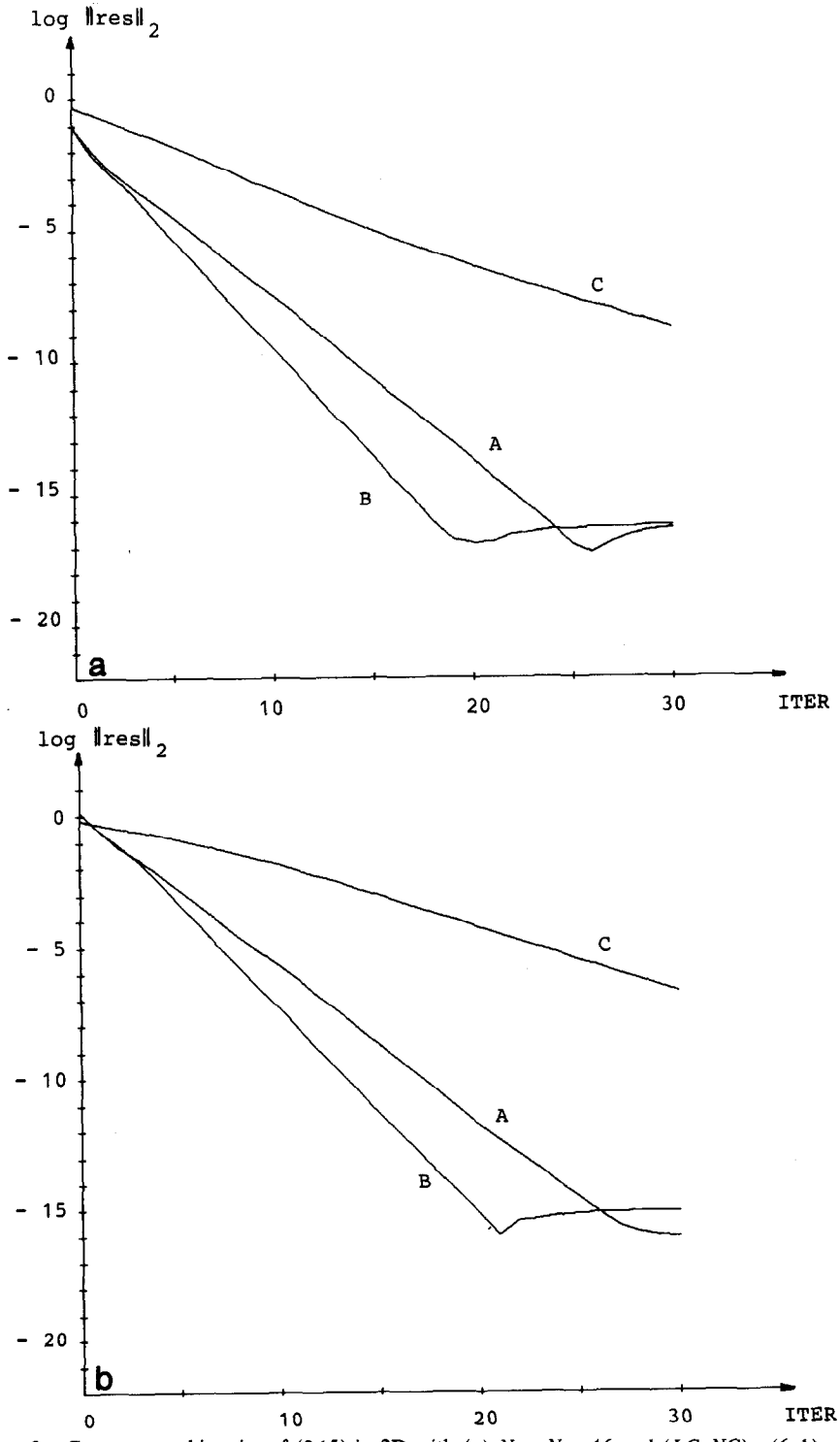

FIG. 3. Convergence histories of (2.15) in 2D with (a) $N_x = N_y = 16$ and $(LC, NC) = (6, 1)$, or (b) $N_x = N_y = 32$ and $(LC, NC) = (8, 1)$. Curves A correspond to $\alpha^k \equiv 1.$, curves B to α^k dynamically chosen according to the MR strategy. Shown is also (curves C) the convergence history using the finite difference preconditioner of [14].

where $\tilde{\mathbf{w}}$ and $\bar{\mathbf{w}}$ are obtained by suitable reorderings of $\mathbf{w}$. Then, starting from arbitrary ξ_0, η_0, and ζ_0, we compute the general step

$$
\begin{aligned}
I_y \otimes I_z \otimes \left(M_x + \frac{\Delta t^{n+1}}{2} A_x \right) \xi^* &= \Delta t^{n+1} M_x \otimes M_y \otimes M_z \mathbf{F} \\
&\quad + I_y \otimes I_z \otimes \left(M_x + \frac{\Delta t^{n+1}}{2} A_x \right) \xi^n \\
&\quad - \Delta t^{n+1} I_x \otimes I_z \otimes A_y \eta^n - \Delta t^{n+1} I_x \otimes I_y \otimes A_z \zeta^n, \\
I_x \otimes I_z \otimes \left(M_y + \frac{\Delta t^{n+1}}{2} A_y \right) \eta^{**} &= I_y \otimes I_z \otimes M_x \xi^* + \frac{\Delta t^{n+1}}{2} I_x \otimes I_z \otimes A_y \eta^n, \\
I_x \otimes I_y \otimes \left(M_z + \frac{\Delta t^{n+1}}{2} A_z \right) \zeta^{n+1} &= I_x \otimes I_z \otimes M_y \eta^{**} + \frac{\Delta t^{n+1}}{2} I_x \otimes I_y \otimes A_z \zeta^n, \\
I_y \otimes I_z \otimes M_x \xi^{n+1} &= I_x \otimes I_y \otimes M_z \zeta^{n+1}, \\
I_x \otimes I_z \otimes M_y \eta^{n+1} &= I_x \otimes I_y \otimes M_z \zeta^{n+1}.
\end{aligned}
\tag{2.26}
$$

Finally, after the last iteration, we recover $\mathbf{w}$ from ζ by solving

$$
\bar{w} = I_z \otimes M_x^{-1} \otimes M_y^{-1} \zeta. \tag{2.27}
$$

Let us assume for the sake of simplicity that $N_x = N_y = N_z = N$. For each ADI iteration, the first sweep requires $3N^2$ independent one-dimensional matrix–vector multiplications and N^2 independent solutions of one-dimensional systems, whereas the second and third sweeps, as well as the two final updates, each require N^2 matrix–vector multiplications and N^2 system solutions. Assuming that all the matrices of the left-hand side of (2.26) are factorized once for all, it turns out that each ADI iteration amounts to performing $12N^2$ one-dimensional matrix–vector multiplications. Recalling that all the one-dimensional matrices involved are tridiagonal, the total cost is about $36N^3$ scalar operations (operation = multiply plus add).

As in the 2D case, a cyclic geometric sequence of parameters $\{\Delta t^n\}$ is chosen. Here, the error reduction factor per cycle cannot be reduced by an arbitrary small amount by increasing the cycle length; however, Douglas [4] has indicated a strategy of choice which leads to a small reduction factor. We recall hereafter the corresponding formulas, referring to [4] for the details. Let $\rho_{\min}$ (resp., $\rho_{\max}$) be a lower (resp., upper) bound for the eigenvalues of the finite element matrix A_{fe} Then, the sequence of parameters is chosen using

$$
\Delta t^n = \frac{2\mu}{\rho_{\min}} \left(\frac{\mu}{\nu} \right)^{n-1}, \qquad n = 1, \ldots, LC, \tag{2.28}
$$

where $\nu > 1$ is a parameter to be chosen, μ is given by $\mu = 3/(1 + 3\nu^2 + \nu^3)$ in terms of ν and LC is the cycle length determined by

$$LC = \text{int}\left[\frac{\log(\rho_{\min}/\rho_{\max})}{\log(\nu/\mu)}\right] + 1. \tag{2.29}$$

Following the optimality criterion proposed in [4], we chose $\nu = 1.78$ and we obtained the error reduction factor per cycle bounded by $R = 0.5029$. We conclude that, for three-dimensional problems, too, it is possible to get an estimate like (2.21), where $\varepsilon = R$ and the cycle length depends logarithmically on N through formula (2.29).

Numerical Results. We present here numerical tests for the 3D problem, where the exact solution is chosen to be $U(x, y, z) = \cos 2\pi x \cdot \cos 2\pi y \cdot \cos 2\pi z$ and $c = 0$ in (2.1). Figure 4 shows the convergence histories of the iterative scheme (2.15) for both fixed ($\alpha^k = 1$) and dynamically chosen acceleration parameters, for two different values of N. The dashed line represents the convergence history of the corresponding 2D problem where the α^k's are chosen dynamically and the cycle length is the same as for the 3D problem. The experiments confirm the good performance of the proposed ADI finite element preconditioner. Note that the cycle length LC given by (2.29) with $\nu = 1.78$ is 6 for $N = 16$ and 8 for $N = 32$. These are precisely lengths we used in the 2D tests in Fig. 3.

2.3. *The Variable Coefficient Case*

The ADI schemes discussed so far can be suitably modified to become ADI preconditioners even for a wide class of variable coefficient problems. For the sake of simplicity, we confine ourselves to the 2D case. We consider the boundary value problem

$$\begin{aligned} -[(aU_x)_x + (bU_y)_y] + cU &= f \qquad \text{in } \Omega \\ U &= \Phi \qquad \text{on } \partial\Omega, \end{aligned} \tag{2.30}$$

where now a, b, and c depend (smoothly) on x and y, and $a(x, y) \geqslant a_0 > 0$, $b(x, y) \geqslant b_0 > 0$, $c(x, y) \geqslant 0$, $\forall x, y \in \Omega$. Again, we are interested in solving (2.30) by an iterative procedure like (2.15). Unless a, b, and c are nearly constant, the finite element preconditioner based on the Helmholtz operator (2.1) will not be efficient. Hence, we have to incorporate the variable coefficients into the ADI preconditioner. This is trivial if each coefficient has a tensor product structure. If this is not the case, i.e., if the dependence of the coefficients upon x and y is general, the tensor product structure of the problem is lost, and one cannot solve exactly the finite element approximation of (2.30) by ADI schemes. However, we are not indeed interested in doing this, but rather in finding a preconditioner for the spectral Chebyshev operator. Thus, taking into account the local character of finite element methods, we propose to "locally" modify the coefficients a, b, and c which appear in the finite element preconditioner, in order to give them a "local" tensor product

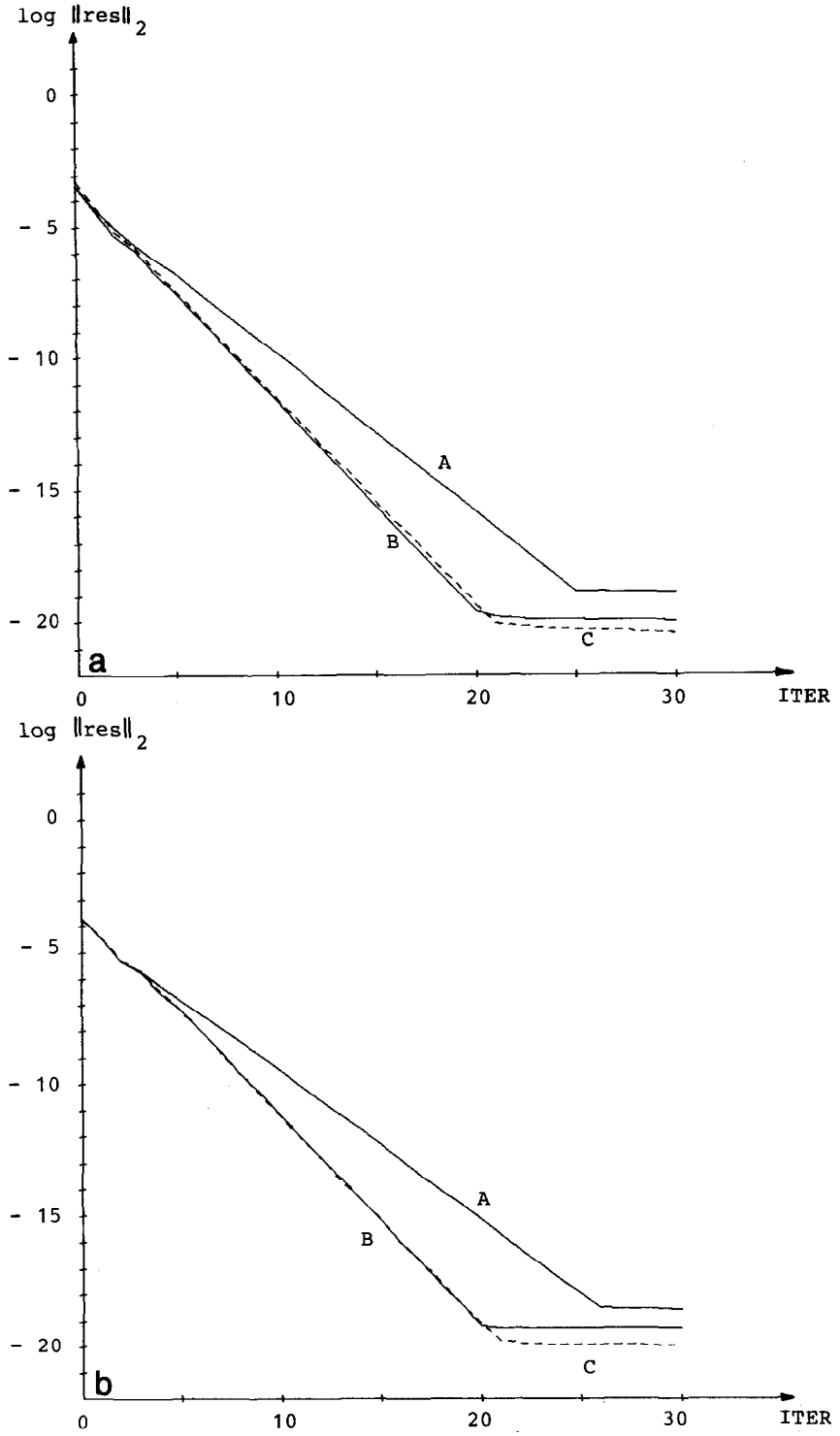

FIG. 4. Convergence histories of (2.15) in 3D with (a) $N_x = N_y = N_z = 16$, or (b) $N_x = N_y = N_z = 32$. Curves A correspond to $\alpha^k \equiv 1.$, curves B to α^k dynamically chosen according to the MR strategy. Shown is also (dashed curves C) the convergence histories of the analogous 2D problem.

structure, which allows the use of an ADI solver. More precisely, let us consider the term $S^{(x)}$ of the stiffness matrix S corresponding to the operator $-(aU_x)_x$. The (ξ_i, ξ_j) node contributes to $S^{(x)}$ with the row

$$(S^{(x)})_{ij,\,kl} = \int_\Omega a(x, y)\, \alpha_i'(x)\, \alpha_k'(x)\, \beta_j(y)\, \beta_l(y)\, dx\, dy, \qquad 1 \leqslant k, l \leqslant N-1. \tag{2.31}$$

Taking into account that $(S^{(x)})_{ij,\,kl} = 0$ if $|l-j| > 1$, we replace (2.31) by

$$(\tilde{S}^{(x)})_{ij,\,kl} = \int_\Omega \tilde{\alpha}^{(j)}(x)\, \alpha_i'(x)\, \alpha_k'(x)\, \beta_j(y)\, \beta_l(y)\, dx\, dy, \tag{2.32}$$

where

$$\tilde{\alpha}^{(j)}(x) = \frac{1}{\text{meas}(B_j)} \int_{B_j} a(x, y)\, dy, \qquad B_j = \text{support of } \beta_j, \tag{2.33}$$

or simply

$$\tilde{\alpha}^{(j)}(x) = a(x, \xi_j). \tag{2.33}'$$

Setting $S_x^{(j)} = \{\int_{-1}^{1} \tilde{\alpha}^{(j)}(x)\, \alpha_i'(x)\, \alpha_k'(x)\, dx\}_{1 \leqslant i,\, k \leqslant N-1}$, then

$$(\tilde{S}^{(x)})_{ij,\,kl} = (S_x^{(j)} \otimes M_y)_{ij,\,kl}. \tag{2.34}$$

The term corresponding to $-(bU_y)_y$ can be dealt with similarly. It is easily seen that the form (2.34) and the corresponding one in the y-direction allow one to use the ADI scheme described in (2.19). A technique of local tensorization based on patches of finite elements in ADI methods was proposed by Hayes [9] in a different context.

As far as the costs are concerned, one has to factorize and store $2N$ one-dimensional matrices ($S_x^{(j)}$, $1 \leqslant j \leqslant N-1$, and $S_y^{(i)}$, $1 \leqslant i \leqslant N-1$) instead of two matrices (S_x and S_y), as for the constant coefficient case. A saving can come by using the same matrix throughout several rows (or columns) of the domain, provided the coefficient varies slowly there.

Numerical Results. We have computed the approximate solution of problem (2.30) with $a = b = 1 + x^2y^2$ and $c = 0$ on a 32×32 mesh, by the method here described. First, we observed very little sensitiveness of the convergence histories on the particular choice (2.33) or (2.33)′ of $\tilde{a}^{(j)}$ in (2.32).

Figure 5 allows us to compare the behavior of the variable coefficient preconditioner to the one of the Laplace preconditioner, showing a superior performance of the former over the latter one. This property becomes more and more evident as long as the total variation of the coefficients increases, although the rates of convergence slow down for both preconditioners.

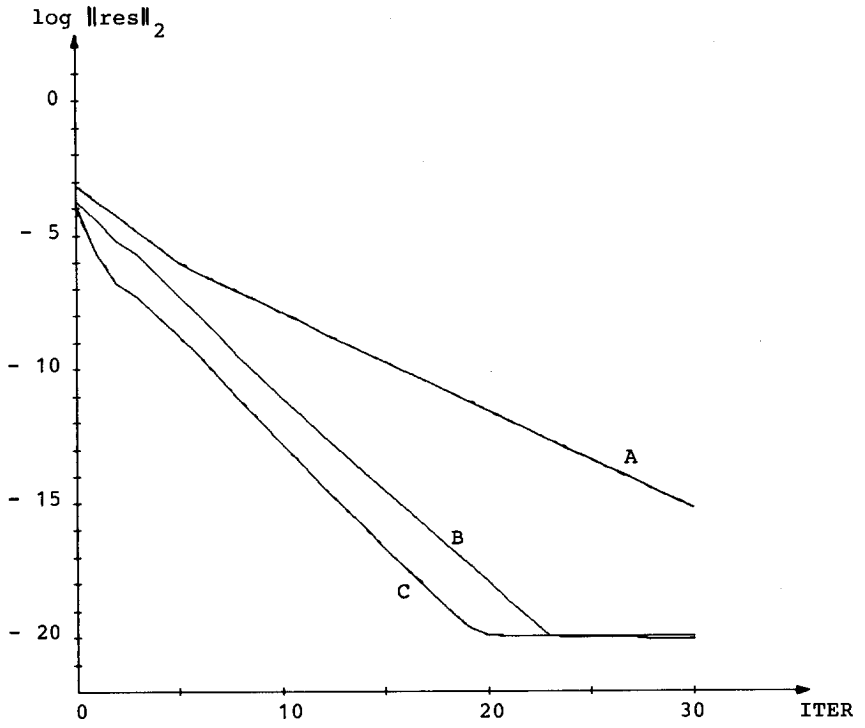

FIG. 5. Convergence histories of the variable coefficient problem (2.30) with $a = b = 1 + x^2y^2$, $c = 0$, $N_x = N_y = 32$, using different preconditioners: the exact finite element scheme for the Laplace operator (curve A), the proposed ADI scheme with modified coefficients for $(LC, NC) = (8, 1)$ (curve B), the exact finite element scheme with modified coefficients (curve C).

3. NEUMANN BOUNDARY CONDITIONS

In this section we discuss iterative methods for solving Chebyshev approximations to Neumann or mixed Dirichlet–Neumann boundary value problems. For the sake of simplicity, we carry out our discussion for the two dimensional domain; the extension to higher dimension is straightforward.

Let us assume that the boundary condition is of the same type (Dirichlet or Neumann) at all the points of a side of the square Ω. Denote by $\partial\Omega_n$ (resp., $\partial\Omega_d$) the collection of sides of Ω where a Neumann (resp., Dirichlet) boundary condition is imposed. We consider the problem

$$\begin{aligned} -\Delta U + cU &= f \qquad \text{in } \Omega \\ \partial U/\partial n &= \Psi \qquad \text{on } \partial\Omega_n \\ U &= \Phi \qquad \text{on } \partial\Omega_d, \end{aligned} \tag{3.1}$$

where $c \geqslant 0$ is a constant and f, Φ, Ψ are given, smooth data.

As usual, the Chebyshev approximation of U is a polynomial $u = u_N \in P_N(\Omega)$ identified through its values at the gridpoints of G_N. At the interior gridpoints we collocate the differential equation

$$[-\Delta u + cu](\xi) = f(\xi) \qquad \forall \xi \in G_N \cap \Omega. \tag{3.2}$$

At a boundary gridpoint which is interior to a side, we impose the proper boundary condition:

$$\frac{\partial u}{\partial n}(\xi) = \Psi(\xi) \qquad \text{if} \quad \xi \in G_N \cap \partial\Omega_n, \tag{3.3.1}$$

$$u(\xi) = \Phi(\xi) \qquad \text{if} \quad \xi \in G_N \cap \partial\Omega_d. \tag{3.3.2}$$

The Dirichlet boundary condition is also enforced at each vertex belonging to a Dirichlet side. Indeed our numerical experiences say that the Dirichlet boundary condition behaves better than the Neumann one, both in terms of final accuracy on the solution and in terms of speed of convergence of the iterative procedure. Finally, at a vertex joining two Neumann sides, there is a potential freedom of choice: one can impose the condition carried by either side. or a linear combination between the two conditions, or even more sophisticated linear relations involving the residual of the partial differential equation at the vertex.

Our idea is to exploit the capability of the finite element method of handling Neumann conditions in a natural way, in order to define the correct boundary condition for the Chebyshev solution through an unambiguous procedure. In other words, among all the possible conditions which can be enforced on the Chebyshev solution at a Neumann/Neumann vertex, we pick up the one suggested by the variational formulation of the finite element scheme used as a preconditioner. It is worth stressing that our approach will not distroy what is commonly referred to as "the spectral accuracy" of Chebyshev methods. Indeed, the final algebraic relations satisfied by our solution at the convergence of the iterative scheme all involve derivatives computed in the usual pseudospectral manner. We set here

$$V_h(\Phi) = \{v_h \in V_h \mid v_h(\xi) = \Phi(\xi) \qquad \forall \xi \in G_N \cap \partial\Omega_d\}; \qquad V_h^0 = V_h(0). \tag{3.4}$$

Let w_h^0 be the finite element approximation of the boundary value problem (3.1), i.e., the solution of the problem

$$w_h^0 \in V_h(\Phi), \qquad \int_\Omega (\nabla w_h^0 \nabla v_h + c w_h^0 v_h) = \int_\Omega f v_h + \int_{\partial\Omega_n} \Psi v_h \qquad \forall v_h \in V_h^0. \tag{3.5}$$

Moreover, given any function $F \in L^2(\Omega)$ and $\eta \in L^2(\partial\Omega_n)$, let us denote by $w_h = A_{fe}^{-1}[F, \eta]$ the finite element solution of the problem:

$$w_h \in V_h^0, \qquad \int_\Omega (\nabla w_h \nabla v_h + c w_h v_h) = \int_\Omega F v_h + \int_{\partial\Omega_n} \eta v_h \qquad \forall v_h \in V_h^0. \tag{3.6}$$

We define a preconditioned Richardson iterative method as follows: The initial point is

$$u^0 = I_N w_h^0, \tag{3.7}$$

whereas the subsequent iterations are defined by the formula

$$u^{k+1} = u^k - \alpha^k I_N A_{fe}^{-1} \left[I_h^0(L_{sp}u^k - f), J_h\left(\frac{\partial u^k}{\partial n} - \psi\right)\right]. \tag{3.8}$$

Here, I_h^0 is the finite element interpolation operator at the interior of the domain, introduced in (2.9). J_h is a (one-dimensional) finite element interpolation operator on the portion of the boundary, where Neumann boundary conditions are prescribed. Precisely, let S be a side of $\partial\Omega_n$, and let Φ be a continuous function on S; define $J_h(\Phi)$ on S by the conditions:

$J_h(\Phi)$ is continuous on $\bar{S}$, piecewise linear between two contiguous grid points of $G_N \cap \bar{S}$, and satisfies:
$J_h(\Phi)(\xi) = \Phi(\xi)\ \forall \xi \in G_N \cap \bar{S}$, unless ξ is a vertex belonging to a Dirichlet side,
$J_h(\Phi)(\xi) = 0$ at a vertex belonging to a Dirichlet side. (3.9)

The last condition corresponds to our choice of enforcing the Dirichlet boundary condition at a vertex where a Dirichlet and a Neumann side meet. Note that the function $J_h(\Phi)$ need not be continuous throughout $\partial\Omega_n$, since it may have jumps at the vertices belonging to two Neumann sides. If the sequence $\{u^k \mid k \in \mathbb{N}\}$ generated by (3.7)–(3.8) converges to a limit polynomial $u^\infty \in P_n(\Omega)$, and the sequence $\{\alpha^k \mid k \in \mathbb{N}\}$ is bounded away from 0, then

$$A_{fe}^{-1}\left[I_h^0(L_{sp}u^\infty - f), J_h\left(\frac{\partial u^\infty}{\partial n} - \Psi\right)\right] \equiv 0,$$

i.e., (see (3.5))

$$\int_\Omega I_h^0(L_{sp}u^\infty - f)\, v_h + \int_{\partial\Omega_n} J_h\left(\frac{\partial u^\infty}{\partial n} - \Psi\right) v_h = 0, \qquad \forall v_h \in V_h^0. \tag{3.10}$$

Taking $v_h = I_h^0(L_{sp}u^\infty - f)$, we get $I_h^0(L_{sp}u^\infty - f) \equiv 0$; i.e., u^∞ satisfies (3.2). Moreover, u^∞ fulfills (3.3.2) because so do all the iterates u^k. Finally, the Neumann boundary condition is translated into the form

$$\int_{\partial\Omega_n} J_h\left(\frac{\partial u^\infty}{\partial n} - \Psi\right)\eta_h = 0 \qquad \forall \eta_n \in T_h, \tag{3.11}$$

where T_h is the space of the restrictions of the functions of V_h^0 to the boundary $\partial\Omega$. Let us give an interpretation to this condition in a pointwise form. If S is a

Neumann side whose vertices are both common with Dirichlet sides, then $J_h(\partial u^\infty/\partial n - \Psi)$ is zero at both vertices and we can choose in (3.11) the function η_h equal to $J_h(\partial u^\infty/\partial n - \Psi)$ on S and to zero elsewhere. This gives $J_h(\partial u^\infty/\partial n - \Psi) \equiv 0$ on S, whence (3.3.1) holds for the gridpoints interior to S. On the contrary, on two or more consecutive Neumann sides, $J_h(\partial u^\infty/\partial n - \Psi)$ need not be identically zero, since this would mean that at each common vertex two Neumann conditions—one for each direction—would be satisfied. What we obtain is that $J_h(\partial u^\infty/\partial n - \Psi)$ is globally "small," in the sense that it is orthogonal to all the test functions in T_h. Taking as a test function a Lagrange basis function concentration at a boundary node, it is easily seen that (3.11) enforces a certain linear combination of the Neumann conditions at three consecutive boundary nodes to be zero.

As for pure Dirichlet boundary conditions, in performing each Richardson step (3.8), we do not compute the finite element correction $A_{fe}^{-1}[F, \eta]$ exactly, but we rather use few sweeps of ADI-iterations, yielding an approximate correction $\mathscr{A}_{fe}^{-1}[F, \eta]$. The ADI-method is the same as the one described in the previous section, with the obvious modifications required by the new boundary conditions.

Finally, the acceleration parameter α^k can be chosen according to the same strategies previously discussed.

Numerical Results. We tested different boundary value problems of the type (3.1) for the exact solution $U(x, y) = \sin 2\pi x \cos 2\pi y$ (which exhibits jumps on the normal derivative at each corner of the domain Ω).

Let the sides of Ω be numbered counterclockwise, starting from the side $\{x = 1\}$. In order to indicate the type of boundary conditions on $\partial\Omega$, we will use the notation $b_1 b_2 b_3 b_4$, where each b_i is D or N depending on whether the Dirichlet or the Neumann boundary condition has been chosen on the side i. The coefficient c in (3.1) was chosen to be either 0 or 1, except in the case of fully Neumann conditions, i.e., $NNNN$, where only $c = 1$ was considered in order to preserve the well-posedness of the problem.

Figure 6a shows the convergence histories of the preconditioned residual

$$\text{res} = \mathscr{A}_{fe}^{-1}\left(I_h^0(L_{sp}u - f), J_h\left(\frac{\partial u}{\partial n} - g\right)\right)$$

for different boundary conditions, $c = 1$ and $N_x = N_y = 32$. The acceleration parameter was $\alpha^k \equiv 1$, and at each Richardson iteration one cycle of ADI steps of length $LC = 8$ was performed. The finite element preconditioner guarantees a good convergence even in the presence of Neumann boundary conditions. Figure 6b shows the results obtained by using the MR strategy in finding the acceleration parameter α^k at each iteration. In all our tests, it was never necessary to artificially prevent α^k from getting too close to 0. The MR strategy becomes progressively less efficient as the number of Neumann sides increases. Yet it yields a better convergence with respect to the fixed parameter strategy, except for fully Neumann conditions. In the latter case, however, the method does not break down, although it is exceedingly slow.

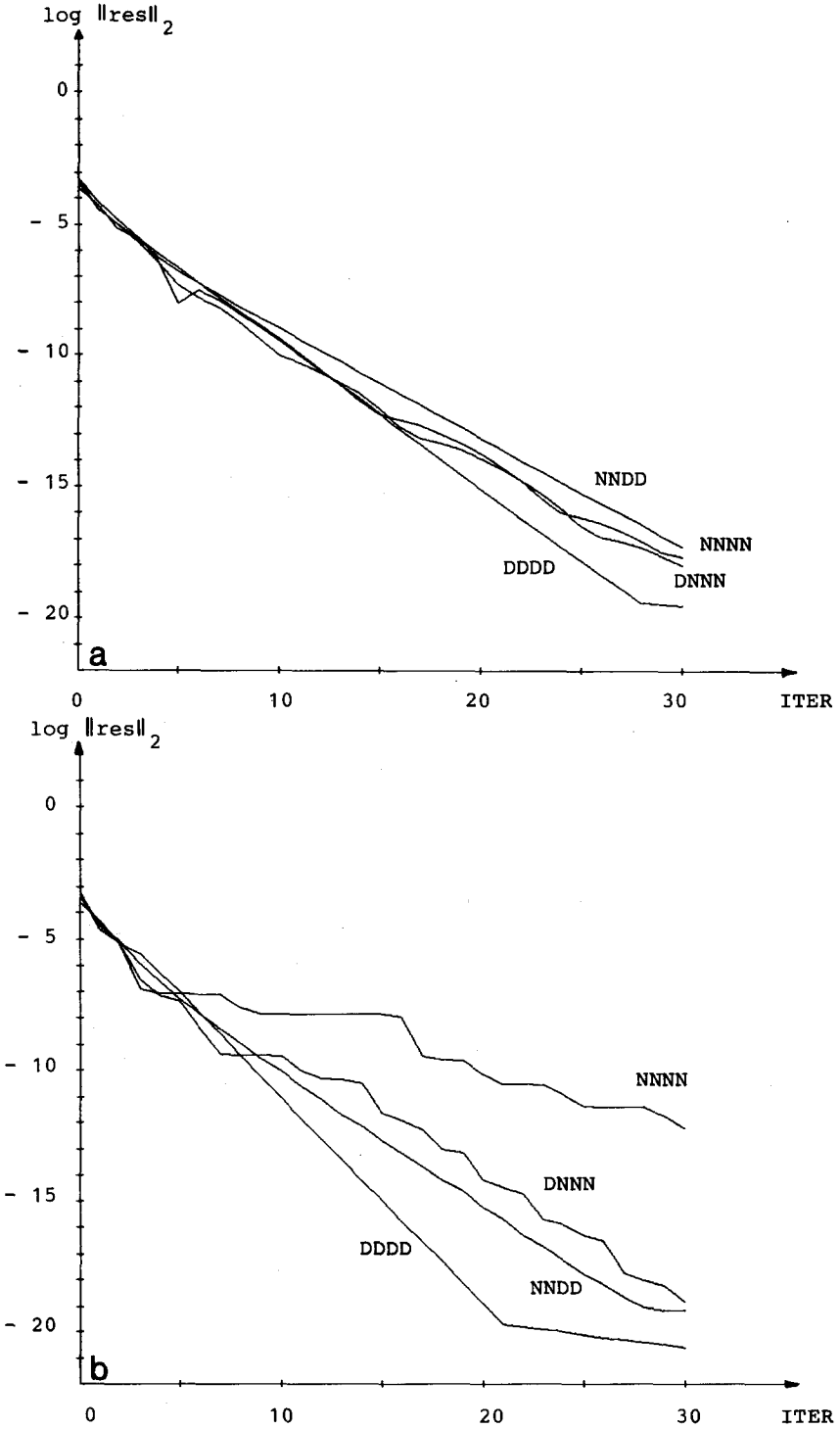

FIG. 6. Convergence histories for the mixed boundary value problem (3.1), with $N_x = N_y = 32$, $(LC, NC) = (8, 1)$ and (a) $\alpha^k \equiv 1.$, or (b) α^k dynamically chosen according to the MR strategy: several combinations of Dirichlet and Neumann boundary conditions.

TABLE I

Relative Errors in the Maximum Norm with the Exact Solution of (3.1), $U(x, y) = \sin 2\pi x \sin 2\pi y$, for Several Combinations of Boundary Conditions

$N_x \times N_y$	*DDDD* ($c=0$)	*NDDD* ($c=0$)	*NDND* ($c=0$)	*NNDD* ($c=0$)	*DNNN* ($c=0$)	*DDDD* ($c=1$)	*NNNN* ($c=1$)
8×8	$0.30\,E-1$	$0.10\,E0$	$0.97\,E-1$	$0.30\,E0$	$0.38\,E0$	$0.30\,E-1$	$0.26\,E0$
16×16	$0.23\,E-6$	$0.54\,E-5$	$0.53\,E-5$	$0.84\,E-5$	$0.10\,E-4$	$0.23\,E-6$	$0.76\,E-5$
32×32	$0.27\,E-14$	$0.54\,E-12$	$0.15\,E-11$	$0.23\,E-11$	$0.30\,E-10$	$0.28\,E-14$	$0.12\,E-11$

In Table I we report the relative errors with the exact solution in the maximum norm, for several combination of boundary conditions and increasing number of gridpoints. For the tested function, the two first digits of the relative error stabilize between the 18th and the 25th iteration, depending upon the boundary conditions. We observe a monotonic loss of accuracy in the computed solution, as the number of Neumann sides increases. This phenomenon is more and more evident as the grid becomes finer and finer. Moreover, it occurs also for the boundary combinations *NDDD* and *NDND*, which have no Neumann/Neumann vertex. Note that for $N_x = N_y = 32$, there is a loss of accuracy of over three orders of magnitude between the case *DDDD* and the case *NDND*! Also recall that in the latter case the computed solution satisfies the exact Neumann boundary condition at each collocation point belonging to a Neumann side. Thus, the phenomenon of the loss of accuracy should not be related to the way we impose the Neumann conditions, but it seems intrinsic to the collocation method.

Finally, let us point out that by a straightforward modification of the operator J_h at the Neumann/Neumann vertices, it is possible to enforce any convex combination of the two Neumann conditions there. Our numerical tests exhibit very little sensitivity to the particular implementation of the Neumann condition at a vertex. As pointed out before, the overall accuracy is determined by the number of Neumann sides. All the implementations are comparable also in terms of speed of convergence of the Richardson iterations, since all of them are based on the variational formulation (3.5) of the finite element preconditioner.

4. Partitioning the Domain

Let us consider problem (3.1) again, under the same conditions. We want to solve it by partitioning the domain Ω into four adjoining subdomains and defining a Chebyshev collocation method on each subdomain, supplemented by suitable matching conditions at the interfaces.

In order to keep the notation as simple as possible, we assume in the following discussion that the domain Ω is divided into four equal domains $\Omega^{(l)}$ ($l = 1, ..., 4$) by the Cartesian axes (see Fig. 7). Let Γ be the union of the internal interfaces between

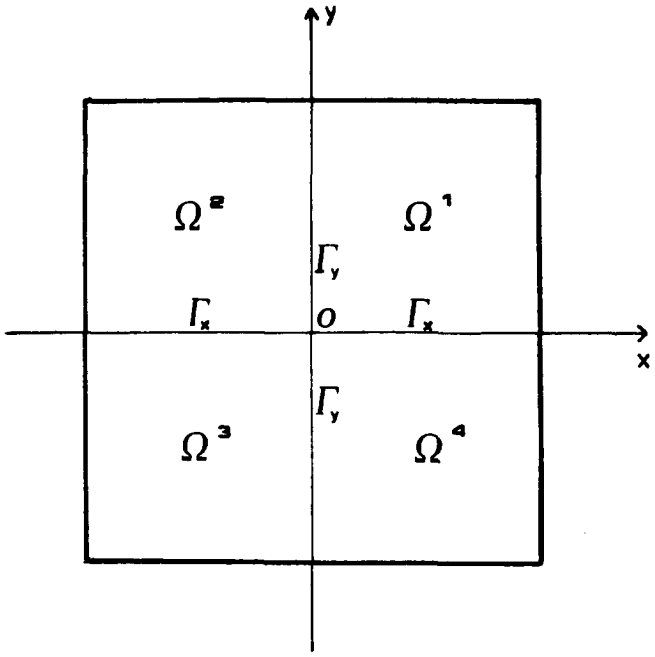

FIG. 7. The decomposition of the domain in four subdomains.

the subdomains, and let $O(0, 0)$ denote the common vertex of the subdomains. We make the further assumption that on two adjoining subdomains the degree of the polynomials in the direction of the common side is the same. Denoting by $N^{(l)} = (N_x^{(l)}, N_y^{(l)})$ the degrees of the polynomials to be used on $\Omega^{(l)}$, we thus assume that

$$N_x^{(1)} = N_x^{(4)}, N_y^{(1)} = N_y^{(2)}, N_x^{(2)} = N_x^{(3)}, N_y^{(3)} = N_y^{(4)}. \tag{4.1}$$

Let

$$G_N^{(l)} = \{\xi^{(l)} = (\xi_i^{(l)}, \xi_j^{(l)}) | 0 \leqslant i \leqslant N_x^{(l)}, 0 \leqslant j \leqslant N_y^{(l)}\} \tag{4.2}$$

be the Chebyshev grid on the domain $\Omega^{(l)}$, obtained from the grid on the reference square $(-1, 1) \times (-1, 1)$ by an affine transformation. By the previous assumption, gridpoints on Γ belong to adjoining domains. We set $G_N = \bigcup_{l=1}^4 G_N^{(l)}$. We look for an approximation $u = u_N$ of the solution U of (3.1) in the space

$$\mathscr{P}_N(\Omega) = \{v \in C^0(\bar{\Omega}) |\ v_{|\Omega^{(l)}} \in P_{N^{(l)}}(\Omega^{(l)}), l = 1, ..., 4\}. \tag{4.3}$$

Thus, u is made-up of four polynomials which match at the gridpoints on Γ, and hence, everywhere on Γ. The function u satisfies the differential equation at the interior Chebyshev points of each subdomain, i.e., (3.2) holds for all $\xi^{(l)} \in G_N^{(l)} \cap \Omega^{(l)}$,

$l = 1, ..., 4$. The boundary conditions are imposed as described in the previous section. At the interface, we have to satisfy a continuity condition which guarantees that the local solutions on each subdomain match to form a global solution on the whole domain. At a smooth interface between two subdomains, this is achieved by requiring the sum of the outward normal derivatives from the two sides to be zero. Thus, at a gridpoint ξ which is interior to a common side between two subdomains $\Omega^{(l)}$ and $\Omega^{(l+1)}$ ($\Omega^{(5)} \equiv \Omega^{(1)}$), we impose

$$\frac{\partial u}{\partial n^{(l)}} + \frac{\partial u}{\partial n^{(l+1)}} = 0. \tag{4.4}$$

At the common corner O, one cannot enforce at the same time the continuity of both the x-derivative and the y-derivative, as the resulting system would be overdetermined. In order to overcome such a difficulty—which is of the same nature of the one encountered in the previous section at a Neumann/Neumann vertex—we resort to a variational formulation of the interface condition, formulated in terms of a finite element preconditioner. Following Deville and Mund [6], we use here a global finite element preconditioner throughout the domain Ω.

Let us describe the details of the method by assuming—for the sake of simplicity—that the boundary conditions in (3.1) are homogeneous Dirichlet. Observe that if U is a continuous function on $\bar{\Omega}$, which solves (3.1) separately on each subdomain $\Omega^{(l)}$, then U satisfies

$$\int_{\Omega} (\nabla U \nabla v + cUv)\, dx\, dy$$

$$= \int_{\Omega} fv\, dx\, dy + \int_{\Gamma_y} \left[\frac{\partial U}{\partial x}\right] v\, dy + \int_{\Gamma_x} \left[\frac{\partial U}{\partial y}\right] v\, dx, \qquad \forall v \in C_0^1(\Omega), \tag{4.5}$$

where $\Gamma_x = \{(x, 0) | -1 < x < 1\}$, $\Gamma_y = \{(0, y) | -1 < y < 1\}$ and $[\partial U/\partial x]$ (resp., $[\partial U/\partial y]$) is the jump of the x-derivative (resp., the y-derivative) of U across Γ_y (resp., Γ_x).

The variational condition

$$\int_{\Gamma_y} \left[\frac{\partial U}{dx}\right] v\, dy + \int_{\Gamma_x} \left[\frac{\partial U}{\partial y}\right] v\, dx = 0 \qquad \forall v \in C_0^1(\Omega) \tag{4.6}$$

is equivalent to the fact that U is the global solution of (3.1) throughout Ω. Therefore, on the discrete level, we are led to enforce the finite element analog of (4.6), where U is replaced by the spectral solution u.

Let V_h^0 denote the space of the continuous functions in Ω, which are piecewise bilinear on the grid G_N defined by (4.1) and which vanish on $\partial\Omega$. Given a function

$F \in L^2(\Omega)$ and two functions $\chi_x \in L^2(\Gamma_x)$, $\chi_y \in L^2(\Gamma_y)$, let $w_h = A_h^{-1}[F, \chi_x, \chi_y]$ denote the solution of the following problem:

$$w_h \in V_h^0, \quad \int_\Omega (\nabla w_h \nabla v_h + c w_h v_h)\, dx\, dy = \int_\Omega F v_h\, dx\, dy + \int_{\Gamma_x} \chi_x v\, dx + \int_{\Gamma_y} \chi_y v\, dy, \quad \forall v_h \in V_h^0. \tag{4.7}$$

Given a function $v \in C^0(\bar{\Omega})$, let $I_h^0 v$ be the function in V_h^0 which coincides with v at the interior gridpoints of each subdomain and which is zero on $\partial\Omega$ *and* on Γ. Furthermore, given a function $\Phi \in C^0(\bar{\Gamma}_x)$, let $J_{h,x}\Phi$ be the continuous, piecewise linear function between two contiguous gridpoints on Γ_x, which coincides with Φ at each interior gridpoints on Γ_x and which vanishes at the endpoints. Let the operator $J_{h,y}$ be defined similarly with respect to Γ_y. Finally, let $I_N v$ denote the function in $\mathcal{P}_N(\Omega)$ which coincides with $v \in C^0(\bar{\Omega})$ at all the gridpoints of G_N.

We define the following Richardson iterative procedure: starting from the initial point $u_0 = I_N w_h^{(0)}$, where $w_h^{(0)} = A_{fe}^{-1}[f, 0, 0]$, set for $k = 0, 1, 2, \ldots$,

$$u^{k+1} = u^k - \alpha^k I_N A_{fe}^{-1} \left[I_h^0 (L_{sp} u^k - f), J_{h,x}\left(\left[\frac{\partial u^k}{\partial y} \right] \right), J_{h,y}\left(\left[\frac{\partial u^k}{\partial x} \right] \right) \right], \tag{4.8}$$

where α^k is a suitable acceleration parameter.

Suppose that the sequence $\{u^k \mid k \in N\}$ generated by (4.8) converges to a limit function $u^\infty \in \mathcal{P}_N(\Omega)$, and that the sequence $\{\alpha^k \mid k \in N\}$ is bounded away from 0. Then, taking into account (4.7), u^∞ satisfies

$$\int_\Omega I_h^0 (L_{sp} u^\infty - f)\, v_h\, dx\, dy + \int_{\Gamma_x} J_{h,x}\left(\left[\frac{\partial u^\infty}{\partial y} \right] \right) v_h\, dx + \int_{\Gamma_y} J_{h,y}\left(\left[\frac{\partial u^\infty}{\partial x} \right] \right) v_h\, dy = 0 \quad \forall v_h \in V_h^0. \tag{4.9}$$

Taking test functions which vanish on Γ and recalling the definition of the interpolation operator I_h^0, it is easily seen that u^∞ satisfies the differential equation at all the interior gridpoints of each subdomain. Thus, (4.9) is reduced to the variational identity

$$\int_{\Gamma_x} J_{h,x}\left(\left[\frac{\partial u^\infty}{\partial y} \right] \right) v_h\, dx + \int_{\Gamma_y} J_{h,y}\left(\left[\frac{\partial u^\infty}{\partial x} \right] \right) v_h\, dy = 0, \qquad \forall v_h \in V_h^0. \tag{4.10}$$

In other words, we enforce the jumps in the normal derivatives across the interfaces to be orthogonal to all the discrete functions on Γ. We call (4.10) the *variational interface condition*. Again, one can interpret this condition as the vanishing of linear combinations of jumps in the normal derivatives, computed at neighboring gridpoints on Γ.

For comparison purposes, we have also considered other ways of imposing the matching of the four spectral solutions at the interfaces. By forcing the interpolation

operator $J_{h,x}$ on Γ_x to be zero at the center O, condition (4.10) splits into two decoupled conditions, i.e.,

$$\int_{\Gamma_x} \tilde{J}_{h,x}\left(\left[\frac{\partial u^\infty}{\partial y}\right]\right) v_h \, dx = 0 \quad \forall v_h \in V_h^0; \qquad \int_{\Gamma_y} J_{h,y}\left(\left[\frac{\partial u^\infty}{\partial x}\right]\right) v_h \, dy = 0 \quad \forall v_h \in V_h^0 \tag{4.11}$$

(where $\tilde{J}_{h,x}$ denotes the modified interpolation operator). By a proper choice of test functions, it is easily seen that (4.11) enforce the jump of the normal derivative to be zero at each collocation point on Γ other than the center, whereas there we have

$$\left[\frac{\partial u^\infty}{\partial x}\right] = 0 \text{ at } O; \qquad \text{no condition on } \left[\frac{\partial u^\infty}{\partial y}\right] \text{ at } O. \tag{4.12}$$

Symmetric conditions can be obtained by modifying $J_{h,y}$ instead of $J_{h,x}$.

A different approach to the interface problem consists of formulating it as a minimization problem. Dihn, Glowinski, and Periaux [7] introduced and discussed this strategy for finite element approximations. Marion and Gay [11] applied the method to spectral approximations, in the case of two adjoining subdomains. We consider here the decomposition of Fig. 7. For the sake of simplicity, we describe the method on the discrete level, although it is possible to formulate it on the exact boundary value problem (3.1). We assume that the physical boundary conditions are homogeneous Dirichlet. Let g be a continuous function on the interface Γ, which is a polynomial of degree N_x on Γ_x and of degree N_y on Γ_y, and which vanishes at the four endpoints of Γ. Let $\mathcal{V}$ denote the finite dimensional space spanned by these functions. For $l = 1, 2, 3, 4$ let $v^{(l)} = v^{(l)}(g) \in P_N(\Omega^{(l)})$ be the Chebyshev collocation approximation to the Dirichlet boundary value problem

$$\begin{aligned} -\Delta v^{(l)} + c v^{(l)} &= f \qquad \text{in} \quad \Omega^{(l)} \\ v^{(l)} &= 0 \qquad \text{on } \partial\Omega^{(l)} \cap \partial\Omega \\ v^{(l)} &= g \qquad \text{on } \partial\Omega^{(l)} \cap \Gamma. \end{aligned} \tag{4.13}$$

Since by definition the polynomials $v^{(l)}$ $(l = 1, ..., 4)$ have a common trace on Γ, they form a global function $v = v(g)$ belonging to $\mathcal{P}_N(\Omega)$ (see (4.3)). Let us introduce the quadratic functional $J: \mathcal{V} \to R$,

$$J(g) = \sum_{\substack{\text{gridpoints} \\ \text{on } \Gamma_x}} \left[\frac{\partial v}{\partial y}\right]^2 + \sum_{\substack{\text{gridpoints} \\ \text{on } \Gamma_y}} \left[\frac{\partial v}{\partial x}\right]^2 \tag{4.14}$$

and let us look for the solution $g_{\min} \in \mathcal{V}$ of the minimization problem

$$J(g_{\min}) = \min_{g \in \mathcal{V}} J(g). \tag{4.15}$$

Finally, take $u = v(g_{\min})$ as the spectral approximation of Problem (3.1). Thus, u

minimizes the jumps of the normal derivative across the interface Γ among all the collocation solutions of the subdomain problems (4.13). The minimization problem (4.15) can be solved by a descent strategy, such as the conjugate gradient method. At each step, the subdomain problems (4.13) are solved, each one independently from the others. Thus, this approach guarantees a high degree of parallelism. Efficient minimization techniques—which include a finite element preconditioned version of the conjugate gradient method—are currently under investigation. The results will be reported elsewhere. Here, we will only compare the minimization approach to other subdomain approaches in terms of accuracy of the solutions. We refer to (4.14), (4.15) as to *the minimality interface condition.*

Numerical Results. First, we focus on the efficiency of the iterative method (4.8). Figure 8 shows the convergence histories of the residual, for a fixed or a dynamically chosen acceleration parameter, when the solution of (3.1) is $U(x, y) = \cos 2\pi x \cdot \cos \pi y$ and $c = 1$. In both cases, we also plotted the convergence history of the single-domain method for the same problem, which uses the same number of total unknowns. The results indicate that the inclusion of the interface integral in the formulation of the finite element preconditioner (see (4.8)) has only a minor effect on the condition number of the problem.

Next, we compare the different strategies of enforcing the continuity condition at the common vertex O. Figure 9 shows the convergence histories corresponding to the variational interface condition (4.10) and to the pointwise condition (4.12). In both cases, we tested the fixed acceleration parameter strategy, as well as the minimal residual strategy. It is clear that the pointwise condition (4.12) leads to a worse conditioned problem than the variational condition: note that the minimal residual strategy breaks down after few iterations. In (4.12) the interface condition is not symmetric in x and y: this results in the undefiniteness of the symmetric part of the preconditioned matrix. On the contrary, the two convergence histories corresponding to the variational interface condition are fairly close to each other and show a constant reduction of the error throughout the iterations. We conclude that the variational interface condition has to be preferred in terms of numerical efficiency.

A comparison in terms of accuracy is presented in Table II. It contains the relative errors in the maximum norm with the exact solution $U(x, y) = \cos 2\pi x \cdot \cos \pi y$ of problem (2.1) with $c = 1$, for different grids and four different interface conditions: the variational condition (4.10), the minimality interface condition (4.15), the pointwise condition (4.12), the symmetric condition in which $[\partial u/\partial y]$ is forced to be zero at O. The minimality condition yields slightly better results, as expected. Conversely, the pointwise condition on $[\partial u/\partial y]$ produces slightly worse results: indeed, the y-derivative of the exact solution at the origin is half the x-derivative there; thus, we force to zero the weaker jump of the approximate solution, instead of the stronger one. However, very little difference among the methods is observed. These results indicate a low sensitiveness of the error to the interface treatment, at least for smooth solutions.

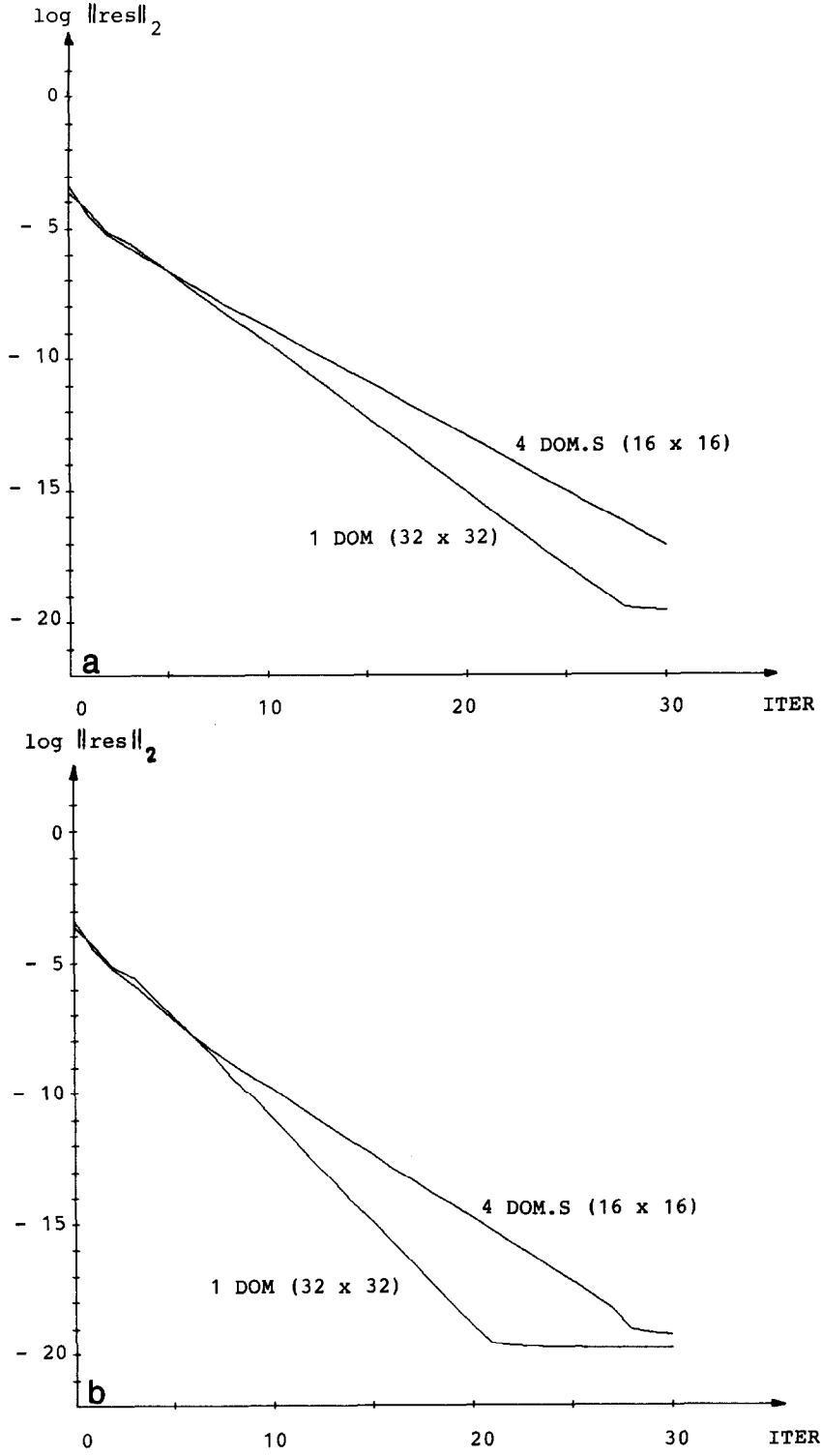

FIG. 8. Convergence histories of the 4-domain and 1-domain iterative methods with ADI parameters $(LC, NC) = (8, 1)$, for (a) $\alpha^k \equiv 1.$, or (b) α^k dynamically chosen according to the MR strategy.

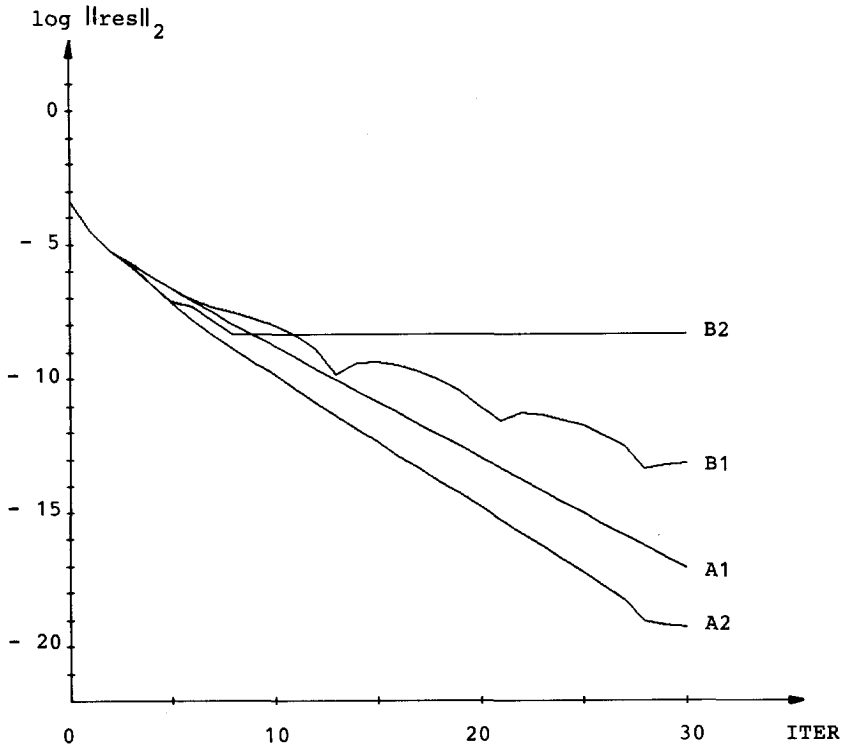

FIG. 9. Convergence histories related to different interface conditions, with $N_x = N_y = 16$ and $(LC, NC) = (8, 1)$. Curve A1: variational interface condition, $\alpha^k \equiv 1.$; curve A2: variational interface condition, α^k dynamically chosen; curve B1: $[\partial u/\partial x] = 0$ at 0, $\alpha^k \equiv 1.$; curve B2: $[\partial u/\partial x] = 0$ at 0, α^k dynamically chosen.

TABLE II

Relative Errors in the Maximum Norm with the Exact Solution of (3.1), $U(x, y) = \cos 2\pi x \cos \pi y$, for Several Interface Conditions

Subdomain grid $N_x \times N_y$	Variational interface condition	Minimality interface condition	$\left[\frac{\partial u}{\partial n}\right] = 0$ at $\Gamma - \{O\}$ $\left[\frac{\partial u}{\partial x}\right]$ at $O = 0$	$\left[\frac{\partial u}{\partial n}\right] = 0$ at $\Gamma - \{O\}$ $\left[\frac{\partial u}{\partial y}\right]$ at $O = 0$
4×4	0.62 $E0$	0.54 $E0$	0.62 $E0$	0.72 $E0$
8×8	0.12 $E-2$	0.10 $E-2$	0.12 $E-2$	0.13 $E-2$
16×16	0.49 $E-10$	0.41 $E-10$	0.49 $E-10$	0.54 $E-10$

TABLE III

Accuracy of the Spectral Domain Decomposition Method; Relative Errors in the Maximum Norm in the Case of Uniformly Structured Solutions of (3.1)

	$u(x, y) = \sin 2\pi x \sin \pi y$	$u(x, y) = \cos 2\pi x \sin \pi y$	$u(x, y) = \cos 2\pi x \cos \pi y$
4 Dom, 4×4	0.14 $E0$	0.54 $E0$	0.62 $E0$
1 Dom, 8×8	0.24 $E-1$	0.33 $E-1$	0.35 $E-1$
4 Dom, 8×8	0.13 $E-3$	0.11 $E-2$	0.12 $E-2$
1 Dom, 16×16	0.23 $E-6$	0.10 $E-6$	0.11 $E-6$
4 Dom, 16×16	0.27 $E-11$	0.43 $E-10$	0.49 $E-10$
1 Dom, 32×32	0.46 $E-14$	0.32 $E-14$	0.38 $E-14$

Finally, let us address the issue of accuracy for spectral domain decompositions. In Table III, the relative errors in the maximum norm with three different test functions are reported. We first observe that the multidomain approach preserves the overall spectral accuracy of the Chebyshev method. However, a comparison with the errors given by the monodomain approach shows a dramatic loss of accuracy. This is due to the poor behavior of the selected test functions at the interface Γ. The function $U(x, y) = \sin 2\pi x \cdot \sin \pi y$ is antisymmetric with respect to both the x-axis and the y-axis. It is easy to check that each iterate u^k produced by the Richardson method (4.8) preserves this property, if the initial guess is itself antisymmetric. Thus, each iterate automatically has zero jump of the normal derivatives at all points on Γ, including the origin. Nonetheless, we see a loss of three orders of accuracy on both the 16×16 and the 32×32 grids. This error is, of course, independent of the way the continuity condition is enforced. The same situation occurs when the test function $U(x, y) = \cos 2\pi x \cdot \sin \pi y$ is used. Since it is antisymmetric in the y-direction, all the Richardson iterates have zero jumps of the y-derivative on Γ_x. Thus, at the limit, (4.10) implies that also the jumps of the x-derivative vanish identically on Γ_y. The errors are even worse than those of the previous case. Finally, the iterate produced by the Richardson method for the test function $U(x, y) = \cos 2\pi x \cdot \cos \pi y$ do have nonzero jumps of their normal derivatives. Our solution satisfies (4.11). For the 8×8 subgrid the jumps range from 10^{-4} at the center to 10^{-6} at the boundaries; for the 16×16 subgrids we observed jumps of order 10^{-11} at the center down to machine accuracy at the boundary. The errors with the exact solution are essentially comparable to those of the second case.

The test functions used so far are smooth and exhibit a uniform structure throughout the domain. Hence, the loss of accuracy observed in the multidomain scheme has to be related to the use of the "local," nonsmooth basis associated with the domain partition, in lieu of the global, smooth basis of the classical Chebyshev

method on the single domain. In order to understand to what extent it is preferable to resort to a domain decomposition as far as accuracy is concerned, we have modified our test functions, by "putting more structure" near a corner of the domain. Precisely, we have considered the functions $U(x, y) = \cos(2\pi\Phi_\gamma(x)) \cdot \cos(2\pi\Phi_\gamma(y))$, with $\Phi_\gamma(s) = [(s+1) + 2^{-\gamma+1}(s+1)^\gamma]/2 - 1$, $\gamma \geqslant 0$. In other words, in each space dimension, we compress the subinterval $[0, 1]$ into the interval $[S_\gamma, 1]$, where $S_\gamma > 0$ is the solution of $\Phi_\gamma(S_\gamma) = 0$. We used two different strategies of domain decomposition: (i) the four domains meet at the origin $O = (0, 0)$ as before, but the subgrid on the northeast domain—where the structure of U concentrates—is allowed to be finer than the other ones; or (ii) the four domains meet at $V_\gamma = (S_\gamma, S_\gamma)$—i.e., there is precisely one full "wave" per domain—but the subgrids carry the same number of points. Table IV reports the relative errors in the maximum norm on Ω, for increasing mesh parameters. In each case, we use an $N_f \times N_f$-grid on the NE domain and an $N_c \times N_c$-grid on the SW domain (the remaining grids are determinted by condition (4.1)). For the single domain method, we use an $(N_f + N_c) \times (N_f + N_c)$-grid; thus, each row in Table IV corresponds to the same total number of unknowns. The results indicate that the single domain scheme is still the most accurate one as long as the solution maintains comparable structures in the different regions of the physical domain (case $\gamma = 2$). Conversely, partitioning the domain may enhance accuracy for nonuniform solutions (case $\gamma = 8$; note that the subinterval $[0.62,1]$ is less than 20% the size of the full interval $[-1, 1]$). Furthermore, only strategy (ii) of domain decomposition leads to acceptable results, indicating the need of a careful choice of the decomposition pattern (let us mention here that alternative approaches, based on the adaptive regridding on the single domain, have recently appeared in the literature (see, e.g. [15, 16])).

TABLE IV

Accuracy of the Spectral Domain Decomposition Method: Relative Errors in the Maximum Norm in the Case of Nonuniformly Structured Solutions of (3.1)

	$\gamma = 2$, $V_\gamma \equiv (0.23, 0.23)$			$\gamma = 8$, $V_\gamma \equiv (0.62, 0.62)$		
N_f, N_c	Single domain	4 domains corner at O	4 domains corner at V_γ	Single domain	4 domains corner at O	4 domains corner at V_γ
4,4	0.77 $E-1$	0.40 $E0$	0.14 $E0$	0.14 $E1$	0.32 $E1$	0.92 $E-1$
8,4	—	0.19 $E0$	—	—	0.15 $E0$	—
8,8	0.81 $E-5$	0.26 $E-2$	0.95 $E-3$	0.92 $E-2$	0.16 $E0$	0.80 $E-4$
16,8	—	0.17 $E-3$	—	—	0.69 $E-3$	—
16,16	0.31 $E-14$	0.23 $E-7$	0.68 $E-8$	0.16 $E-6$	0.67 $E-3$	0.12 $E-7$
32,16	—	0.57 $E-9$	—	—	0.16 $E-9$	—

5. Conclusions

We have investigated several issues related to the use of finite element preconditioners in solving Helmholtz equations by spectral collocation methods.

First, we confirm that finite elements exhibit performance superior to that of finite differences in preconditioning spectral methods, as first shown by Deville and Mund [6] (see also [7]). The new point here is that the superior performance is maintained, at lower cost, if the direct finite element solver is suitably replaced by an iterative approximate solver. We have chosen ADI iterations because they enjoy the same tensor product structure as spectral methods and they are easily amenable to parallel implementation. Of course, other fast solution techniques of the finite element discretization could be used instead.

Next, we indicate a correct and efficient way of enforcing Neumann boundary conditions by exploiting the variational formulation of finite elements. The speed of convergence of the iterative scheme is moderately affected by the presence of Neumann sides, and the scheme never breaks down. On the other hand, we observe a loss of accuracy in the spectral collocation solution whenever Neumann boundary conditions are enforced. The approximation error decays at the same rate as the one corresponding to pure Dirichlet boundary conditions, but the former one remains larger than the latter one by some orders of magnitude.

Finally, we show how to take advantage of the variational formulation of finite elements to enforce the patching conditions in a spectral multidomain method. Cross-points can be easily handled by our formulation. Concerning the accuracy of spectral multidomain solutions, we observe that it may not be wise to adopt a domain decomposition approach for the exclusive purpose of parallelization (i.e., for assigning each subdomain to a different processor). If the solution is expected to have comparable smoothness throughout the physical domain, it is convenient to keep the computational domain as large as possible, in order to get the maximum accuracy assured by the global expansion of spectral methods. Parallelism can be better exploited in the process of solving the resulting algebraic system (a discussion of the possible strategies of parallelization of spectral methods can be found in [1]). Of course, partitioning the domain is unavoidable in non-cartesian geometries and is highly recommended when the solution has different structures in different regions of the physical domain.

Appendix A

In the following, we go back to the ADI-finite element preconditioner introduced in Section 2 for the 2D case. Our aim is to prove, in the simplified case of periodic boundary conditions, that the condition number of the matrix $\mathscr{A}_{fe}^{-1} L_{sp}$ is bounded independently of the mesh parameters N_x and N_y, provided the ADI cycle length is increased at a logarithmic rate in the mesh parameters. Thus, the basis functions

will be trigonometric polynomials, and the collocation points will be equally spaced in the domian. For the sake of simplicity, we consider the problem

$$-\Delta U = f \qquad \text{in} \quad \Omega = (0, 2\pi)^2$$
$$U \qquad 2\pi\text{-periodic in } x \text{ and } y.$$

Moreover, we normalize U by the condition $\int_\Omega U\,dx\,dy = 0$. Let L denote the matrix corresponding to the Fourier collocation approximation of this problem at the uniform grid $\{\theta_{mj} = (m\pi/N,\ j\pi/N) | 0 \leqslant m,\ j \leqslant 2N-1\}$. The preconditioning matrix A is obtained by approximating the same problem via bilinear finite elements on the same grid. $\mathscr{A}^{-1}$ will denote the matrix obtained by applying to the finite element problem one cycle of the ADI procedure described in Section 2. The matrices L and A have the same set of eigenvectors $\{\mathbf{s}_{kl} | -N \leqslant k,\ l \leqslant N-1,\ k, l \neq 0\}$, where

$$\mathbf{s}_{kl}(\theta_{mj}) = e^{i(km+lj)(\pi/N)},\ 0 \leqslant j, m \leqslant 2N-1.$$

The eigenvalue of L corresponding to the eigenvector $\mathbf{s}_{kl}$ is $\lambda_{kl} = k^2 + l^2$, whereas the eigenvalue of A is

$$\rho_{kl} = 6\left\{\frac{1-\cos(k\pi/N)}{2+\cos(k\pi/N)} + \frac{1-\cos(l\pi/N)}{2+\cos(l\pi/N)}\right\}\frac{N^2}{\pi^2}.$$

Let $\sigma_{kl} = \rho_{kl}^{-1}\lambda_{kl}$ be the eigenvalue of the matrix $A^{-1}L$. It is easy to check that

$$0.69 \leqslant \sigma_{kl} \leqslant 1, \qquad -N \leqslant k, l \leqslant N-1. \tag{A.1}$$

It follows that the condition number $\kappa(A^{-1}L)$ of $A^{-1}L$ satisfies

$$\kappa(A^{-1}L) < 1.45. \tag{A.2}$$

We recall that if A is the matrix of the finite difference preconditioning, one has for the same boundary value problem $\kappa(A^{-1}L) < 2.45$. Thus, the finite element approach yields a better preconditioning property for spectral systems. We shall prove that $\tilde{\kappa} = \text{cond}(\mathscr{A}^{-1}L)$ is itself bounded independently of N, provided that the cycle length LC of the ADI procedure is chosen properly. To this end, let $\tilde{\sigma}_{kl}$ be the eigenvalue of $\mathscr{A}^{-1}L$ corresponding to the eigenvector $\mathbf{s}_k$.

PROPOSITION 1. *Let κ be the condition number of $A^{-1}L$, and let $\tilde{\kappa}$ be the condition number of $\mathscr{A}^{-1}L$. Given a cycle length LC of the ADI procedure* (2.19), *there exists ε, with $0 \leqslant \varepsilon < 1$ and ε dependent on LC, such that*

$$\tilde{\kappa} = (1-\varepsilon)^{-1}\kappa. \tag{A.3}$$

Proof. First, note that ρ_{kl} splits in the sum $\rho_{kl}=\rho_k+\rho_l$, where ρ_k, ρ_l are the eigenvalues of the one-dimensional finite element matrix. Then observe the relation between $A^{-1}\mathbf{s}_{kl}$ and $\mathscr{A}^{-1}\mathbf{s}_{kl}$,

$$\mathscr{A}^{-1}\mathbf{s}_{kl}=A^{-1}\mathbf{s}_{kl}-(1/\rho_{kl})\,E\mathbf{s}_{kl}, \tag{A.4}$$

where E denotes the operator which advances the error between the exact solution of the finite element problem and the one computed by ADI through a parameter sequence of length LC. It is known (see [13]) that the error reduction on a single eigenfunction $\mathbf{s}_{kl}$ is represented by the formula

$$E\mathbf{s}_{kl}=\varepsilon_{kl}\mathbf{s}_{kl}, \qquad \text{with} \quad \varepsilon_{kl}=\varepsilon(\rho_k,\rho_l,LC)=\prod_{n=1}^{LC}\frac{1-\Delta t^n\rho_k}{1+\Delta t^n\rho_k}\frac{1-\Delta t^n\rho_l}{1+\Delta t^n\rho_l}, \tag{A.5}$$

where $\{\Delta t^n\}$ is the set of parameters of the ADI procedure. It is obvious that

$$0\leqslant\varepsilon_{kl}<1. \tag{A.6}$$

Now, (A.4) and (A.5) imply

$$\mathscr{A}^{-1}L\mathbf{s}_{kl}=\rho_{kl}^{-1}\lambda_{kl}(1-\varepsilon_{kl})\,\mathbf{s}_{kl},$$

whence

$$\tilde{\sigma}_{kl}=(1-\varepsilon_{kl})\,\sigma_{kl}, \tag{A.7}$$

Due to (A.7) and (A.6), there exists a constant $\varepsilon=\varepsilon(LC)$, with $0\leqslant\varepsilon<1$, such that

$$\sigma_{\min}(1-\varepsilon)\leqslant\tilde{\sigma}_{kl}\leqslant\sigma_{\max}, \tag{A.8}$$

where $\sigma_{\min}$, $\sigma_{\max}$ denote the minimum and the maximum eigenvalue of $A^{-1}L$. (A.8) implies immediately (A.2). Thus Proposition 1 is proven.

In (A.3), ε might become arbitrarily close to 1 as N increases, so that our iterative scheme might break down. This is not the case if the parameter sequence $\{\Delta t^n\}$ is chosen following the strategy of [13] and the cycle length LC is $O(\log_2 N)$. We recall that the range $[\rho_{\min},\rho_{\max}]$ of the eigenvalues ρ_k, $k=-N,\ldots,N-1$, is divided in nonuniform intervals I_n, in such a way that exists Δt^n satisfying

$$\left|\frac{1-\Delta t^n\rho}{1+\Delta t^n\rho}\right|\leqslant\sqrt{\varepsilon}, \qquad \forall\rho\in I_n. \tag{A.9}$$

In this way, after one cycle, each eigenvector is reduced by a factor at least ε (see (A.5)). The resulting cycle length LC satisfies

$$\left(\frac{1-\sqrt{\varepsilon}}{1-\sqrt{\varepsilon}}\right)^{2LC}\simeq\rho_{\max}/\rho_{\min}. \tag{A.10}$$

Recalling that $\rho_{\max}/\rho_{\min} = O(N^2)$, we obtain

$$\sqrt{\varepsilon} \simeq \frac{LC_{\sqrt{N-1}}}{LC_{\sqrt{N+1}}}. \tag{A.11}$$

Thus, if $LC \simeq \log_2(N)$, ε is bounded independently of N. Proposition 1 and (A.11) allow us to state the final result.

PROPOSITION 2. *Let κ be the condition number of $A^{-1}L$, and let $\tilde{\kappa}$ be the condition number of $\mathscr{A}^{-1}L$. If the cycle length LC of the ADI procedure defined by* (2.19) *satisfies $LC = O(\log_2 N)$, there exists a constant ε, bounded independently of N, with $0 \leqslant \varepsilon < 1$, such that*

$$\tilde{\kappa} = (1-\varepsilon)^{-1}\,\kappa. \tag{A.12}$$

ACKNOWLEDGMENT

The authors thank the referees for suggesting several improvements in the quality of the paper.

REFERENCES

1. C. CANUTO, "Parallelism in Spectral Methods," Int. Symposium on Vector and Parallel Processors for Scientific Computation, Academia Nazionale dei Lincei, Rome, September 1987.
2. C. CANUTO, M. H. HUSSAINI, A. QUARTERONI, AND T. A. ZANG, *Spectral Methods in Fluid Dynamics* (Springer-Verlag, New York, 1988).
3. C. CANUTO AND A. QUARTERONI, *J. Comput. Phys.* **60**, 315 (1985).
4. J. DOUGLAS, JR., *Numer. Math.* **4**, 41 (1962).
5. J. DOUGLAS, JR. AND T. DUPONT, "Alternating-Direction Galerkin Methods on Rectangles," in *Numerical Solution of Partial Differential Equations II*, edited by B. Hubbard (Academic Press, New York, 1971), p. 133.
6. M. DEVILLE AND E. MUND, *J. Comput. Phys.* **60**, 517 (1985).
7. Q. V. DIHN, R. GLOWINSKI, AND J. PERIAUX, "Solving Elliptic Systems by Domain Decomposition Methods with Applications," in *Elliptic Problem Solvers II*, edited by G. Birkoff and A. Schoenstradt (Academic press, New York, 1984), p. 395.
8. D. FUNARO, Thesis, University of Pavia, 1981 (unpublished).
9. L. J. HAYES, *SIAM J. Numer. Anal.* **18**, 627 (1981).
10. P. HALDENWANG, G. LABROSSE, S. ABBOUDI, AND M. DEVILLE, *J. Comput. Phys.* **55**, 115 (1984).
11. Y. MARION AND B. GAY, "Resolution des equations de Navier–Stokes par methode pseudo-spectrale via une technique de coordination," Sixieme Colloque International "Simulation d'écoulement par elements finis," Antibes, France, June 1986.
12. S. A. ORSZAG, *J. Comput. Phys.* **37**, 70 (1980).
13. D. W. PEACEMAN AND H. H. RACHFORD, JR., *SIAM J. Numer. Anal.* **3**, 28 (1955).
14. Y. S. WONG, T. A. ZANG, AND M. Y. HUSSAINI, *Comput. Fluids* **14**, 85 (1986).
15. A. BAYLISS AND B. MATKOWSKY, *J. Comput. Phys.* **71**, 147 (1987).
16. A. BAYLISS, D. GOTTLIEB, B. MATKOWSKY AND M. MINKOFF, *J. Comput. Phys.* **81**, 421 (1989).
17. M. DEVILLE AND E. MUND, "Finite Element Preconditioning for Pseudospectral Solutions of Elliptic Problems," manuscript in preparation.
18. N. N. YANENKO, *The Method of Fractional Steps* (Springer-Verlag, Berlin, 1971).